Manuscript prepared for Atmos. Chem. Phys.
with version 4.2 of the LaTeX class copernicus.cls.
Date: 9 January 2013

Quantifying the impact of BOReal forest fires on Tropospheric oxidants over the Atlantic using Aircraft and Satellites (BORTAS) experiment: design, execution and science overview

Paul I. Palmer[1], Mark Parrington[1], James D. Lee[2], Alistair C. Lewis[2], Andrew R. Rickard[3,4], Peter F. Bernath[2,5], Thomas J. Duck[6], David L. Waugh[7], David W. Tarasick[8], Stephen Andrews[9], Eleonora Aruffo[10,11], Loren J. Bailey[6], Edward Barrett[1], Stephan J.-B. Bauguitte[12], Kevin R. Curry[6], Piero Di Carlo[10,11], Lucy Chisholm[7], Lin Dan[13], Grant Forster[14], Jonathan E. Franklin[6], Mark D. Gibson[15], Debora Griffin[13], Detlev Helmig[16], James R. Hopkins[2], Jason T. Hopper[6], Michael E. Jenkin[17], David Kindred[18], Jenny Kliever[13], Michael Le Breton[19], Stephan Matthiesen[1], Michael Maurice[13], Sarah Moller[2], David P. Moore[20], David E. Oram[14], Sebastian J. O'Shea[19], R. Christopher Owen[21], Camille M.L.S. Pagniello[6], Steven Pawson[22], Carl J. Percival[19], Jeffrey R. Pierce[6], Shalini Punjabi[9], Ruth M. Purvis[2], John J. Remedios[20], Kaja M. Rotermund[6], Kimiko M. Sakamoto[6], Arlindo M. da Silva[22], Kevin B. Strawbridge[8], Kimberly Strong[13], Jonathan Taylor[19], Robert Trigwell[1], Keith A. Tereszchuk[9], Kaley A. Walker[13], Daniel Weaver[13], Cynthia Whaley[13], and Jennifer C. Young[3]

[1]School of GeoSciences, University of Edinburgh, Edinburgh, UK
[2]National Centre for Atmospheric Science (NCAS), Department of Chemistry, University of York, York, UK
[3]National Centre for Atmospheric Science (NCAS), School of Chemistry, University of Leeds, UK
[4]now at the National Centre for Atmospheric Science (NCAS), Department of Chemistry, University of York, York, UK
[5]now at the Department of Chemistry & Biochemistry, Old Dominion University, Norfolk, VA, USA
[6]Department of Physics and Atmospheric Science, Dalhousie University, Halifax, Nova Scotia, Canada
[7]Meteorological Service of Canada, Dartmouth, Nova Scotia, Canada
[8]Environment Canada, Toronto, Ontario, Canada
[9]Department of Chemistry, University of York, York, UK
[10]Center of Excellence CETEMPS, University of LAquila, LAquila, Italy
[11]Department of Physical and Chemical Sciences, University of L'Aquila, L'Aquila, Italy
[12]Facility for Airborne Atmospheric Measurements, Bedford, UK
[13]Department of Physics, University of Toronto, Toronto, Ontario, Canada
[14]National Centre for Atmospheric Science (NCAS), School of Environmental Sciences, University of East Anglia, Norwich, UK
[15]Department of Process Engineering and Applied Science, Dalhousie University, Halifax, Nova Scotia, Canada
[16]Institute of Arctic and Alpine Research, University of Colorado, Boulder CO, USA
[17]Atmospheric Chemistry Services, Okehampton, Devon, EX20 1FB, UK
[18]U.K. Meteorological Office, Exeter, UK
[19]School of Earth, Atmospheric and Environmental Sciences, University of Manchester, Manchester, UK
[20]Department of Physics and Astronomy, University of Leicester, Leicester, UK
[21]Department of Geological and Mining Engineering Sciences, Michigan Technological University, MI, USA
[22]Global Modeling and Assimilation Office, NASA Goddard Space Flight Center, MD, USA

Correspondence to: Paul Palmer
(pip@ed.ac.uk)

Abstract. We describe the design and execution of the BORTAS (Quantifying the impact of BOReal forest fires on Tropospheric oxidants using Aircraft and Satellites) experiment, which has the overarching objective of understanding the chemical aging of airmasses that contain the emission products from seasonal boreal wildfires and how these airmasses subsequently impact downwind atmospheric composition. The central focus of the experiment was a two-week deployment of the UK BAe-146-301 Atmospheric Research Aircraft (ARA) over eastern Canada. The planned July 2010 deployment of the ARA was postponed by 12 months because of activities related to the dispersal of material emitted by the Eyjafjallajökull volcano. However, most other planned model and measurement activities, including ground-based measurements at the Dalhousie University Ground Station (DGS), enhanced ozonesonde launches, and measurements at the Pico Atmospheric Observatory in the Azores, went ahead and constituted phase A of the experiment. Phase B of BORTAS in July 2011 included the same measurements, but included the ARA, special satellite observations and a more comprehensive measurement suite at the DGS. Integrating these data helped us to describe pyrogenic plumes from wildfires on a wide spectrum of temporal and spatial scales. We interpret these data using a range of chemistry models, from a near-explicit gas-phase chemical mechanism to regional and global models of atmospheric transport and lumped chemistry. We also present an overview of some of the new science that has originated from this project.

1 Introduction

The Quantifying the impact of BOReal forest fires on Tropospheric oxidants over the Atlantic using Aircraft and Satellites (BORTAS) experiment was conducted during July-August 2010 and 2011 (phases A and B, respectively) funded by the UK Natural Environmental Research Council, with meteorological field support from the UK Meteorological Office and Environment Canada. The overarching objective of BORTAS was to better understand the chemical evolution of plumes emitted from the burning of biomass, with a particular emphasis on the net production of tropospheric ozone (O_3), and downwind impacts on air quality. Our sub-objectives include: i) sample biomass burning outflow from boreal North America over the western boundary of the North Atlantic during summer 2011 using the UK BAe-146-301 Atmospheric Research Aircraft; ii) describe observed chemistry within plumes by using the measurements to constrain a near-explicit chemical mechanism, with particular attention to the NO_y and organic chemistry; iii) derive a reduced chemical mechanism suitable for a global chemistry transport model (CTM) that accurately describes chemistry within the plumes; iv) quantify the impact of boreal forest fires on oxidant chemistry over the temperate and subtropical Atlantic using a nested 3-D CTM, driven by a reduced version of the near-explicit chemical mechanism and by assimilated field measurements; and v) detect, validate and quantify the impact of boreal biomass burning on global tropospheric composition using data from space-borne sensors. To address these objectives, BORTAS integrated a number of concurrent activities:

1) airborne in situ measurements, 2) space-borne measurements, 3) balloon, ground-based in situ and remote-sensed measurements in Canada and the Azores, 4) near-explicit tropospheric chemical modelling, 5) regional and global chemistry transport models, and 6) inverse models. This paper provides an overview of BORTAS-B with an emphasis on the summer measurement campaign; BORTAS-A was described by Parrington et al. (2012).

Over the past 20 years (1990-2011), Canadian forest fires have burned a median of 1.7 million hectares/year, ranging from 626,000 hectares in 2001 to over 7 million hectares in 1995 (data from Natural Resources Canada), with a year to year variability partly explained by large-scale changes in climate (e.g., the El Niño Southern Oscillation). Although this is a small fraction of the forested land (0.1-1.8%), it represents a substantial input of carbonaceous material and trace gases released to the atmosphere. The predominant tree species (by volume) includes coniferous spruce (53%) and pine (9%) and broad-leaf poplar (12%), which determines the distribution of natural emission of biogenic volatile organic compounds but also the release of volatiles as part of pyrolysis associated with forest fire (Drysdale, 2008).

Tropospheric O_3 is a regulated secondary air pollutant because at elevated concentrations it is linked with human respiratory illness and damage to vascular plants with implications for food production and biogeochemical cycling. A considerable body of work has shown that long-range transport of O_3 and its photochemical precursors can represent a significant contribution to background O_3 over downwind continents and in some circumstances result in an increased number of days that exceed the regulated threshold concentration. The role of seasonal wildfires on this long-range transport of pollution remains unclear, partly because of its large year-to-year variability and partly because there remains substantial uncertainty in our understanding of the chemistry within these plumes. The primary focus of BORTAS was to understand the production and loss of O_3 within plumes emitted from boreal forest fires as they are transported across the North Atlantic towards Europe.

Figure 1 shows a simplified schematic of the general atmospheric chemical system (Atkinson and Arey, 2003) that is the focus of BORTAS. We start on the left hand side with an emitted volatile organic compound (VOC) being oxidized by a common atmospheric oxidant OH, NO_3 or O_3, resulting in the production of an alkyl radical R that rapidly reacts with molecular oxygen to form peroxy radicals (HO_2, RO_2). The fate of peroxy radicals depends on the photochemical environment. In a pyrogenic environment, where levels of nitrogen oxides ($NO+NO_2=NO_x$) are significantly elevated above ambient concentrations, RO_2 typically proceeds via the RO_2+NO and RO_2+NO_2 routes. RO_2+NO proceeds via two channels resulting in the production of alkyl nitrates ($RONO_2$) and/or the production of RO and NO_2, which can lead to the formation of O_3 via NO_2 photolysis. RO_2+NO_2 can also lead to the formation of $ROONO_2$. Here, we focus on the peroxy acyl nitrates, denoted as PANs, where RO_2 is R'C(O)OO. PAN is thermally stable at temperatures lower than $<$263 K, typical of the free and upper troposphere, resulting in an atmospheric lifetime of months so that it

can be transported over long distances; in contrast, the lifetime of PAN in the lower troposphere (>287 K) is minutes to hours. The most abundant PANs in the troposphere is the eponymous peroxyacetyl nitrate (PAN, $CH_3C(O)O_2NO_2$) and peroxypropionyl nitrate (PPN, $CH_3CH_2(O)O_2NO_2$) with PAN representing 75–90% of the total PAN concentration. PAN is effectively a thermally controlled reservoir for reactive nitrogen delaying subsequent chemistry. Previous studies have shown that RO_2+HO_2 is still a significant sink of RO_2 in a pyrogenic environment, producing peroxides (H_2O_2 and hydroperoxides, ROOH), with H_2O_2 readily removed by wet deposition. ROOH, which is much less soluble than H_2O_2, has an atmospheric lifetime of 2–3 days and can produce alkoxy radicals (via photoysis) and produce aldehydes and recycle RO_2 via OH oxidation. A recent review of chemistry measurements of pyrogenic plumes highlights that, based on the enhancement ratio of $\Delta O_3/\Delta CO$ (a common, brute-force metric for characterizing O_3 production), there is no canonical theory of O_3 chemistry within plumes (Jaffe and Wigder (2012) and references therein). This is not surprising given the combined effects of large variations in, for example, fuel type/loading, combustion efficiency (and subsequent emitted VOC amounts), meteorological and photochemical environments (e.g., convective energy, and aerosol and cloud characteristics), and the age of the measured plumes on the chemical system.

The impetus for BORTAS was a small number of pyrogenic airmasses originating from northern Canada and Alaska that were intercepted during the 2004 UK International Transport of Ozone and Precursors (ITOP) measurement campaign, which was part of the larger International Consortium for Atmospheric Research on Transport and Transportation (ICARTT). The main focus of ICARTT was to characterize the air quality over the North Atlantic, with an emphasis on long-range transport of anthropogenic pollution. The pyrogenic airmasses were identified by a distinct distribution of primary chemical markers (CO, ethene, acetlyene, and benzene), accompanied by elevated concentrations of PAN (Lewis et al., 2007). Analysis of these airmasses revealed no robust relationship between CO and O_3. In a case study, one pyrogenic plume, sampled at three different locations as it travelled across the North Atlantic, showed a net increase (17 ppb) in O_3 and a concurrent decrease in CO over the five-day period. A Lagrangian model, used to understand the responsible chemical processes as the plume travelled over the North Atlantic, highlighted the role of aerosol in slowing both the production and loss of O_3 but found the plume remained chemically active mainly driven by the thermal decomposition of PAN as it descended through the free troposphere (Real et al., 2007). They also found that the model reproduced the change in $\Delta O_3/\Delta CO$ (negative to positive) over the North Atlantic confirming that the change in O_3 was due to photochemistry rather than dilution. The BAe-146 aircraft payload during BORTAS, described below, included instruments to better speciate the NO_y budget and characterize aerosols, including semi-volatiles.

The NASA Arctic Research of the Composition of the Troposphere from Aircraft and Satellites (ARCTAS) 2008 campaign included a science objective on quantifying emissions from boreal forest fires and the near-field chemical evolution of the fire plumes (Jacob et al., 2010). During the Spring

(April) phase over Alaska they intercepted Alaskan air masses (3-8 days old) and found evidence of O_3 production, but during the Summer phase (June–July) over western Canada they sampled mainly young, near-field plumes ($<$ 1day) and evidence supporting net O_3 production was inconclusive. During the summer phase they showed that 40% of the NO_x was converted to PAN within a few hours of emission thereby limiting the immediate reactivity within the plume (Alvarado et al., 2010). Model analyses of these data concluded that forest fire plumes have little impact on the median O_3 profile over Canada (Alvarado et al., 2010). During BORTAS, owing to large-scale fires in northwest Ontario, we were able to sample pyrogenic plumes with a range of photochemical ages providing us with an excellent opportunity to understand the photochemical aging processes within these plumes.

This paper describes the experimental design of the BORTAS-B airborne campaign which was conducted during 12th July–3rd August, 2011. This includes an overview of BORTAS-B incorporating a description of the fire activity and meteorology (section 2) for the time period; a detailed description of the ground-based, airborne, and space-borne instruments that supported the BORTAS-B campaign (section 3); a description of first results (section 4) from individual research groups from the BORTAS-B science team, including a description of the modelling strategy that is the subject of individual papers. We conclude in section 5.

2 Campaign Overview

To determine the optimal time and location of the measurement campaign we used the GEOS-Chem atmospheric chemistry transport model driven by NASA GEOS-5 reanalysis meteorology (section 3.5) to study the atmospheric transport of year-specific biomass burning emissions over Canada, acknowledging substantial year-to-year variations in the emissions and transport pathways. Based on that analysis we identified late July as the period that would give us the largest probability of intercepting near-field (within Canada) and far-field (e.g., from boreal Asia) plumes. We also identified Halifax Nova Scotia as the optimal locus for our base of operations for the BAe-146 ARA, giving us access to long-range transported plumes at high latitudes and near-field plumes that tend to remain close to the latitude of emission. As we discuss below, choosing Halifax also provided us with an opportunity to work with the ground-based measurement community, which greatly enhanced the science return of the campaign.

BORTAS has four major elements: Canadian ground-based network, BAe-146 Atmospheric Research Aircraft (ARA), satellite observations, and the computer modelling of atmospheric chemistry and transport, all of which contribute to the science objectives of the campaign and are discussed in detail below.

BORTAS was originally planned for Summer 2010 but the BAe-146 ARA was grounded for civil contingency flying associated with the dispersal of volcanic aerosol from the eruption of Eyjafjallajökull (Dacre et al., 2012). We decided to run the campaign as planned (12th July –3rd August,

2010) but without the ARA, providing an important dry-run for the modelling and ground-based measurement teams; we hereinafter refer to this as Phase A of the campaign (BORTAS-A). Deployment of the ARA in 2011 during 12th July–3rd August is Phase B of BORTAS (BORTAS-B) and is the main subject of this paper.

2.1 Fire Activity

Figure 2 shows the time and location of active fires over the Northern Hemisphere during Phases A and B of BORTAS. In many respects, the number and distribution of July fires over high northern latitudes during 2010 were closer to the decadal mean than 2011 with the exception of fire activity over Russia. During 2011 there was substantially less burning over Chukotka and Kamchatka federal subjects of Russia. Fires over Canada during BORTAS-B were comparatively early, with large wildfires near Richardson Backcountry and Slave Lake, Alberta, starting in May, which removed some of the combustible material in that area that would have typically burned later in the summer (see 2010 vs 2011). BORTAS-B was largely characterized by a small number of large near-field fires over Northwestern Ontario which started and completed during the campaign and substantial far-field fires from boreal Asia. Tree species over this region includes pine (*Pinus banksiana*, *Pinus resinosa*, *Pinus strobus*), spruce (*Picea glauca*, *Picea mariana*), poplar (*Populus basalmifera*), aspen (*Populus grandidentata*, *Populus tremuloides*), maple (*Acer rubrum*), fir (*Abies balsamea*), birch (*Betula papyrifera*), ash (*Fraxinus nigra*), and tamarack (*Larix laricina*).

2.2 Meteorological Overview for BORTAS-A and BORTAS-B

The climatological flow pattern in the Northern Hemisphere troposphere in summer indicates that pollutants generally follow a west to east flow pattern, often increasing in forward speed as they depart the east coast of North America and head toward the European continent. This feature of transport over the North Atlantic is regulated by the location and strength of the polar vortex and the mid-North Atlantic subtropical high. We present the synoptic meteorology and accompanying atmospheric transport that occurred during the BORTAS-B field intensive and discuss it in context with BORTAS-A and the climatological mean for the same period. Table 1 provides a brief description of the meteorology associated with each BORTAS-B flight.

Mid-troposphere flow patterns

Figure 3a shows the climatological (1979–1995) mid-tropospheric flow (500 hPa) for North America for the period 15th July–3rd August, which is similar to the first two weeks of July and shows a trough over Hudson Bay across Quebec to Greenland and Iceland. Figure 3d shows that the 2010 flow was similar to the climatological pattern with only weak positive anomalies in height over North America and stronger positive anomalies with ridging off the west coast of Canada and over European Russia and far eastern Siberia and Kamchatka. This is in contrast to the BORTAS-B

period 3g, with strong positive anomalies in geopotential height over the upper Mississippi, the North Pacific and a dramatic positive height anomaly over Eastern Siberia. A positive anomaly also lay over the mid-North Atlantic covering all of Greenland possibly resulting in a more northerly route for the North Atlantic transport to the European continent. Labrador and Maritime Canada had negative anomalies along with Alaska and British Columbia. The Maritime Canada negative anomaly is indicative of the cooler and cloudy weather that occurred during BORTAS-B.

Lower troposphere flow patterns

Figure 3b shows the climatology mean 850 hPa surface during the BORTAS period. The pattern maintains ridging over the NE Pacific, the subtropical anticyclone over the mid North Atlantic, with a minor trough from a low in northern Davis Strait to the northern Labrador Sea. Figure 3e shows that the anomaly for 2010 has strong positive variation over NE Pacific, weak negative over central Quebec with an extension to Northwestern Ontario and just South of Newfoundland and East of Nova Scotia. Figure 3h shows that for 2011 there are stronger negative anomalies to the Southeast of Nova Scotia, south of Sable Island with a trough to Hudson Bay then extending west to northern Saskatchewan to the upper Mackenzie Valley to Yukon. A slight positive anomaly lay to the south of the Great Lakes again indicative of the surface and upper ridging that favoured the development of forest fires in Northwestern Ontario.

Surface flow patterns

Figure 3c shows the climatological mean sea level pattern over North America for the BORTAS period, which shows a weak pressure pattern with a few isobars due to continued ridging associated with the subtropical anticyclone off the western North Atlantic and the ridge over the Northeast Pacific, and a low over Baffin Island with a weak trough to the central and western US. Figure 3f shows that the anomaly pattern for 2010 has a strong high over the Northeast Pacific off British Columbia and a low pressure area south of Newfoundland with a trough to Northwestern Ontario then along the tree line to Great Slave Lake, Northwest Territories. Figure 3i shows that a more dramatic anomaly pattern in 2011 with lower pressure south of Newfoundland and east of Nova Scotia, a low on southern Baffin Island and a significant negative anomaly over Yukon and Northwest Territories to Northwestern Ontario. A potential result of the pattern for 2011 is that more synoptic low pressure systems transited from west to east than is the norm. In summary, the surface synoptic pattern for 2011 commenced with an area of high pressure in the earlier portion of the study then quickly gave way to the intrusion of frontal troughs, weak low pressure systems and shifts of wind from the southwest to the west and northwest. A respite from this dynamic pattern occurred on 29th July as a short-lived ridge moved across Atlantic Canada.

3 BORTAS-B Measurements

3.1 BAe-146 Aircraft Payload and Deployment

The BAe-146 aircraft has an endurance of approximately 5.5 hours with a full science payload (4.2 tons) and has a science speed of 200 knots Calibrated Airspeed (103 m/s CAS), resulting in a standard air range of approximately 2000 km at sea level, increasing to 3,300 km at a typical maximum working standard pressure altitude (sHp) of 30,000 ft (9.1 km); for A-to-A flights with varying altitudes and time on station this typically gave a working radius of about 900 km, and for A-to-B science flights a range of about 1800 km. Table 2 shows the BAe-146 instrument payload during BORTAS-B. The payload reflects the core science objectives of characterizing the chemical processing of pyrogenic airmasses with measurements of total alkyl nitrates, total peroxy nitrates, total NO_y, NO, NO_2, and PAN.

Before entering the BORTAS in-theatre domain the aircraft transited from Cranfield UK (where it is based) to Horta, Azores on the 12/7/11; from Horta, Azores to St John's, Newfoundland on the 13/7/11; from St John's, Newfoundland to Halifax on the 13/7/11. Figure 4 shows the 13 non-transit BORTAS-B flights and the location of active ozonesonde launch sites (Table 3) and Along-Track Scanning Radiometer (ATSR) firecounts. With the exception of flight B624 when there was no Light Induced Fluorescence (LIF) NO_y data, all instruments were operational and reported data for all flights shown. Table 1 summarizes each BORTAS-B flight, including outbound and inbound transit legs; a total of 77 hours, 28 mins, and 33 secs. The BAe-146 spent most of the time sampling in the free troposphere, with more than a third of the time between 6 and 9 km.

3.2 Dalhousie Ground Station (DGS) and Additional Canadian Sites

Wherever possible we coordinated surface measurements with the BORTAS-B aircraft deployment to improve understanding of the transport of pyrogenic plumes as they travelled over Canada. The DGS represents a coordinated measurement activity conducted at a height of 65 m on the roof of the Sir James Dunn building at Dalhousie University (44.64° N, 63.59° W), including investigators from Dalhousie University, Environment Canada, University of Toronto, and University of Sherbrooke. Table 4 summarizes the individual instruments that participated in the DGS activity during BORTAS-B. BORTAS flight B623 explictly included profile measurements around the DGS. Some of the DGS science activities are briefly discussed below.

The University of Toronto Atmospheric Observatory (TAO), located at 43.66°N, 79.40°W and 174 m a.s.l. on the 16th floor of the Burton Tower of the McLennan Physical Laboratories in downtown Toronto, including in particular an ABB Bomem DA8 FTIR Spectrometer (Wiacek et al., 2007) similar to the instrument housed at Dalhousie University. Work within BORTAS-B led by DGS investigators have found instances where pyrogenic plume pass over both the TAO and DGS, providing an opportunity to study the chemical evolution of a plume (Griffin et al., 2012; Franklin et al., 2012).

We worked closely with Environment Canada to coordinate additional launches of ozonesondes that could help characterize the vertical distribution of O_3 associated with pyrogenic plumes. Table 3 shows the key launch sites during BORTAS-B; for interest Table 3 also shows the corresponding launches for 2010 which were supporting another measurement intensive to understand stratosphere-troposphere exchange (Bourqui et al., 2012). The 2010 ozonesonde data were used to help evaluate the GEOS-Chem atmospheric chemistry transport model (Parrington et al., 2012) as part of modelling activities supporting BORTAS-B.

BORTAS investigators also used data from the Canadian Operational Research Aerosol Lidar Network (CORALNet) led by Environment Canada (Strawbridge, 2012) with sites at Egbert (Ontario), Sherbrooke (Quebec) and Acadia (Nova Scotia). These sites were chosen to monitor transport events as well as investigate regional air quality issues. For further information about the Lidar technology the reader is referred to Strawbridge (2012)

3.3 Pico Atmospheric Observatory

The Pico Mountain station (also known as PICO-NARE) is located in the Azores, Portugal (38° 28.226″ N, 28° 24.235″ W, 2225 m a.s.l.). Its geographical location makes it ideal to study the long-range free-tropospheric transport of pyrogenic plumes from boreal North America (Honrath et al., 2004), and provides us with opportunity to study aged plumes after they have travelled partway across the North Atlantic. Table 5 shows the measurements taken during BORTAS phase A and B. As part of the outbound and inbound transit flights the BAe-146 ARA encircled PICO-NARE in an attempt to cross-calibrate similar measurements.

Figure 5 shows a typical FLEXPART "retroplume" during July 2011 when elevated CO at Pico was attributed to biomass burning. We only include a brief description of this calculation here, referring the reader to Honrath et al. (2008) for a detailed discussion. Each retroplume represents the mean of the backward transport of thousands of individual particles, with each particle affected by convection, dispersion and advection. The plume calculation, driven by $1^\circ \times 1^\circ$ ECMWF meteorology, is initialized every three hours centred on Pico station over the altitude 2–2.5 km above sea level. The residence times of the particles were normalized by the air density in each cell to account for difference in air density along the back trajectories to yield the specific volume weighted residence time (SVWRT). The SVWRT was convolved with time-dependent emission inventories for anthropogenic (Olivier and Berdowski, 2001) and burning biomass (Mu et al., 2011) CO sources. Values reported in Figure 5 represent the residence time, scaled by the maximum value in the meridional direction and vertically integrated, such that a non-dispersive plume could be 100% from the point of emission to the receptor location. During July 2011 the atmospheric flow over the BORTAS-B region was such that variations of CO at Pico from Canadian pyrogenic sources were not as prominent as previous years.

3.4 Satellite Observations

Validating space-borne observations associated with wildfires was a core science objective of BORTAS-B, allowing us to relate the relatively small-scale data from the BAe-146 aircraft to larger spatial scales and longer temporal scales. During the campaign near-real time satellite data were used to inform deployment of the BAe-146 aircraft.

We used near-real time measurements from the Michelson Interferometer for Passive Atmospheric Sounding (MIPAS) (Fischer et al., 2008) aboard the Envisat satellite and the Infrared Atmospheric Sounding Interferometer (IASI) (Clerbaux et al., 2009) aboard the MetOp satellite to help us intercept pyrogenic plumes with the aircraft during BORTAS-B. MIPAS measures atmospheric limb emission spectra 14.5–4.1μm at a spectral resolution of 0.0625 cm^{-1} since January 2005 over a tangent altitude range 6–68 km and is in a polar sun-synchronous orbit with a local solar time of 10:00 and a 35-day repeat cycle. MIPAS observations were specially planned to coincide with BORTAS-B flights. IASI uses an infrared Fourier Transform (FTIR) spectrometer to measure spectra 15.5–3.62μm at a spectral resolution of 0.5 cm^{-1} and is in a polar sun-synchronous orbit with a local solar time of 09:30 and a 29-day repeat cycle. We used MIPAS products developed by the University of Leicester, including CO, PAN, acetylene, formic acid, ethane, and acetone (Moore and Remedios, 2010; Parker et al., 2010; Moore et al., 2012; Illingworth et al., 2011), which have been shown previously to be markers of wildfires (Alvarado et al., 2010). The IASI near-real-time CO data product was provided by C. Clerbaux (CNRS/INSU, LATMOS-IPSL, Paris, France) and P.-F. Coheur (Université Libre de Bruxelles, Brussels, Belgium) (Clerbaux et al., 2009; George et al., 2009). We also used IASI products developed by the University of Leicester, including CO, formic acid, and acetylene, with detection products for these compounds and also ethene, ammonia, and HCN. Figure 6 shows an example of how these detection products were used in BORTAS-B to understand the spatial extent of biomass burning plumes. The data show a distinct CO plume over eastern Canada on 19th July 2011, derived from the difference in brightness temperature between 5μm and 10μm, which also corresponds to elevated concentrations of formic acid.

We also used data from the Atmospheric Chemistry Experiment (ACE) (Bernath et al., 2005; Tereszchuk et al., 2011) which is a high-resolution FTIR spectrometer that measures spectra 750 to 4400 cm^{-1} with a resolution of 0.02 cm^{-1}. ACE aboard SCISAT-1, which is in a 74° inclination circular orbit, can measure up to 30 sunrise and sunset occultations per day with a vertical resolution of 2–3 km from 150–5 km in cloud-free scenes. A number of trace gases are retrieved from the ACE spectra that are elevated in wildfires e.g., CO, acetonitrile, formic acid, formaldehyde, acetylene, ethane, methanol (Tereszchuk et al., 2011, 2012). Figure 7 shows IASI total column CO for 2/8/11, with a black symbol superimposed denoting the location of an ACE occultation profile from which we show a profile of HCN and PAN down to 7 km. Both PAN and HCN show elevated concentrations suggesting this enhancement is due to the biomass burning outflow shown by IASI.

In collaboration with colleagues at the NASA Jet Propulsion Laboratory we requested special

"step-and-stare" observations from the Tropospheric Emission Spectrometer (TES) (Beer et al., 2001) aboard the Aura spacecraft with a repeat cycle of 16 days. TES is a high-resolution imaging FTIR spectrometer that observed spectral radiance in the range 650–3050 cm^{-1} at a resolution of 0.1 cm^{-1}. It has an instrument field-of-view at the surface of 8×5 km^2. Data from this instrument has been used previously to study boreal wildfires over Sibera (Verma et al., 2009) and Canada (Alvarado et al., 2010). The BORTAS-B step-and-stare TES observations effectively increased the spatial density of measurements over eastern Canada during BORTAS-B and subsequently increased the number of coincident profile measurements.

Figure 8 shows a comparison between an O_3 profile measured from the BAe-146 during its descent into Thunder Bay airport, Ontario on 26th July 2011 and a colocated O_3 profile retrieved by TES on the same date separated by approximately 30 km and 4 hours. Figure 8a shows the raw 1-second aircraft O_3 measurement, the TES retrieval and its prior, and the aircraft profile smoothed by the TES averaging kernels. The prior for the TES O_3 retrieval has been scaled to the aircraft profile, and the retrieved O_3 profile has been adjusted to this scaled prior, following Kulawik et al. (2008); Rodgers and Connor (2003). The aircraft profile was smoothed with the TES averaging kernels by (i) removing repeat measurements at the same vertical level, (ii) appending the scaled prior to extend it into the stratosphere, and (iii) interpolating it to the TES vertical pressure grid. Figure 8b shows the averaging kernels for the retrieved O_3 profile. The O_3 profile measured from the BAe-146 showed relatively low (20-40 ppb) mixing ratios between the surface and 750 hPa with a relatively thick layer of enhanced O_3 extending from 700 to 400 hPa with mixing ratios of 50-80 ppb. The prior profile used in the TES retrieval was scaled to match the O_3 mixing ratio measured from the aircraft at the highest pressure level (approximately 350 hPa). Between the surface and this pressure level the scaled prior is representative of background tropospheric O_3 mixing ratios (red dotted line in Figure 8a). The TES O_3 profile (red solid line in Figure 8a) showed a similar vertical distribution to the aircraft profile with mixing ratios of 20-40 ppb below 750 hPa, similar to the prior, increasing to approximately 60 ppb at 400 hPa. The averaging kernels in Figure 8b indicate that this retrieval was not sensitive to O_3 at the lowest pressure levels of the profile but was sensitive to the pressure levels with the observed O_3 enhancement. At higher pressure levels (lower altitudes), the TES profile showed good agreement with the raw aircraft measurements. Comparison against the aircraft profile smoothed with the TES averaging kernels, however, indicated that the TES retrieval overestimated the O_3 profile in the middle troposphere by up to 20 ppb.

3.5 Model and Data Forecast Products

The main forecasting products for BORTAS-B included 1) NASA GEOS-5 (Global Earth Observing System) forecasts of carbon monoxide emitted boreal biomass burning (latitudes $>50^\circ$), in collaboration with Global Modelling and Assimilation Office at NASA Goddard; and 2) Environment Canada meteorological forecasts together with operational output from the air quality model GEM-

MACH (Global Environmental Multi-scale-Modelling Air quality and CHemistry). We also used forecasts from the UK Meteorological Office and the European Centre for Medium-range Weather Forecasts, and used the HYbrid Single-Particle Lagrangian Integrated Trajectory (HYSPLIT) model (Draxler, 1999) to locate the origin of plumes observed by the aircraft.

As part of the deployment planning we used near-real time fire data from: 1) Natural Resources Canada http://cwfis.cfs.nrcan.gc.ca/en_CA/fwmaps/fdr; 2) emission data from the Fire Locating And Monitoring of Burning Emissions (FLAMBE) which incorporates fire data from geostationary and polar orbiting satellite (Reid et al., 2009); and 3) fire products from the NASA Moderate-Resolution Imaging Spectroradiometer (MODIS) instruments from the Fire Information for Resource Management System (FIRMS) via the NASA Earth Observing System Data and Information Service. This information is independent to the Quick Fire Emission Dataset (QFED) developed by NASA and used by the GEOS-5 CO forecasts (Rienecker et al., 2008; Ott et al., 2011). CO total column and profile data from IASI (described above), available $<$3 hours after measurements, was also used for plume tracking and flight planning during BORTAS.

4 First results and science overview

The BORTAS-B airborne campaign delivered a rich dataset to better understand chemistry in biomass burning plumes, partly serendipitously because of the timing and location of fires over Northwestern Ontario during our Halifax-based deployment. We are still in the early stages of interpreting these data but our results have already revealed new insights, some of which we briefly describe here and refer the reader to dedicated papers.

Intercepting pyrogenic plumes is non-trivial but we found that GEOS-5 CO fields reliably forecasted the general spatial distribution of the plumes, allowing us to accordingly deploy the BAe-146. Figure 9 shows the GEOS-5 CO forecast for B624 on the 21st July 2011, which showed pyrogenic plumes in the mid-lower troposphere over Newfoundland Island and the Gulf of St. Lawrence. The flight pattern was designed to maximize time within the plume and explore the vertical dimension. These aircraft observations serve to illustrate the rapid horizontal and vertical gradients associated with the plume. Figure 10 shows that these plumes indeed travel as thin, coherent filaments with a vertical dimension of the order of 100 m, in agreement with previous studies, reflecting possibly vertical wind shear where the material was first lofted into the atmosphere. As part of BORTAS we are parameterizing time-dependent forecast skill of the GEOS-5 CO fields using optical flow methods (Keil and Craig, 2009), which is the subject of an upcoming paper (Matthiesen et al., 2012). Associated with these filamental structures were rapid gradients in O_3 across the plume boundaries, in agreement with previous studies of near-field powerplant plumes that showed a non-linear response to levels of NO_x (Ryerson et al., 2001).

For BORTAS science studies we have collectively chosen to use CO, with some combination of

biomass burning tracers acetonitrile (CH_3CN) and hydrogen cyanide (HCN), to identify biomass-burning plumes. By virtue of the primary science objective of BORTAS, the resulting airborne data are biased to biomass burning plumes so that we cannot use the mean statistics of these data to identify plumes, an approach adopted by other campaigns. Instead, we have used measurements from a single flight (B625, 7/24/11, Figure 4) during which we sampled almost exclusively concentrations representative of the background atmosphere: mean and median values were lower than those derived from all the data, and there was no significant statistical relationship between CO and CH_3CN. Even in the background atmosphere, we expect a distribution of trace gas concentrations. Here, we define a plume that has a value greater than the 99th percentile ($\simeq$mean+3 standard deviations) of the B625 data. For CO, CH_3CN, and HCN these 99th percentile threshold values are 148 ppb (n=237), 150 ppt (n=236), and 122 ppt (n=118), respectively. Combining these constraints will improve the confidence of identifying a plume. This admittedly crude statistical analysis helps to justify our method of plume identification and provides a definition for all subsequent BORTAS science studies.

Figure 11 shows significant contributions of total CO from biomass burning regions during the BORTAS-B period, as depicted by the tagged version of the GEOS-Chem global 3-D model (Parrington et al., 2012). The model is driven by uncorrected FLAMBE biomass burning emission estimates, which are known to have a positive bias. At the surface over eastern Canada, where BORTAS-B took place, the largest contribution to CO is from Siberia (as it is indeed for the rest of the Northern hemisphere), with substantial contributions from East and West Canada and the Southwest and Eastern United States. In the free troposphere, where the aircraft spent most of its time, the background is dominated by Siberian burning with near-field variations also from East and West Canada. Particularly strong Siberian burning episodes were observed on 28th July using IASI CO data, although enhanced CO amounts were detected over this region throughout the BORTAS-B period. A more detailed treatment of the emission and transport of biomass burning emission will the subject of a future study.

Emissions from open biomass burning (i.e., incomplete combustion) still represent largely CO_2 and H_2O but also include CO and a suite of organic compounds. The relative abundance of these organic species depends on the phase of the fire (flaming or smouldering). The co-emission of these organic compounds along with CO has been reported extensively and the correlation of these with CO and with dry mass of biomass burnt has been used to derive emission ratios (ER) and emission factors (EF); see for example Andreae and Merlet (2001). During BORTAS-B we determined a wide range of emission ratios for organic compounds (expressed as ppt[NMHC] per ppb[CO]) using data from whole air samples analysed on the ground using GC-FID and in flight for selected species using PTR-MS. Derived ER values during BORTAS-B (Lewis et al., 2012) agreed very well for many species with earlier experiments over a similar geographic region (Simpson et al., 2011), providing confidence in subsequent analysis involving the scaling-up of these measurements using CO fire

emission estimates and a global 3-D chemistry transport model. In particular, the BORTAS-B ERs have been used to determine the extent to which biomass burning contributes to the global distribution of species such as benzene, ethene, propene and toluene, which are traditionally thought of as mainly anthropogenic tracer whose regulation has seen a continued decline in developed countries. Analysis using the GEOS-Chem chemistry transport model shows that in many remote locations biomass burning can be the dominant hydrocarbon source (Lewis et al., 2012).

Pyrogenic emissions of many simple non-methane hydrocarbons (NMHCs) and small oxygenated compounds such as methanol and acetone are now well established but larger polar and semi-volatile species are less well characterized. These species have lower vapour pressures than simple non-methane hydrocarbons so that if they transported under cool free troposphere conditions they can partition to the aerosol phase. Laboratory studies (e.g., Christian et al. (2004)), and near-field measurements (e.g., Yokelson et al. (2008)) of forest burning biomass show that a range of higher carbonyl compounds are released and there is some evidence of enhanced emissions of monoterpenes and longer chain aliphatic compounds. However, detection of these compounds in the field, and in particular in plumes undergoing long-range transport, is analytically difficult. They are often not amenable to sampling and storage in whole air sampling canisters because of wall and O_3 losses, and the complexity of isomers makes PTR-MS an unsuitable technique for individual speciation. BORTAS-B provided the first flight opportunities for a fast response in-flight GC-MS designed specifically for C_5-C_{12} VOCs including oxygenated compounds and monoterpenes. Intercepted boreal biomass burning plumes in the mid-troposphere showed that species such as furfural, benzaldehyde, benzonitrile, acetophenone and benzoic acid were present in significant abundances and that downwind fire plumes also showed elevated higher hydrocarbons such as naphthalene and monoterpenes including alpha pinene, camphene, beta-pinene, 3-carene limonene and eucalyptol. ERs for these species from aged plumes have been determined and their phase partitioning estimated for a range of plume temperatures. The addition of an in-flight GC-MS to BORTAS-B also provided additional discrimination to PTR-MS data, in particular providing a quantitative measurement of the relative abundance of furan and isoprene species that give a combined response by PTR-MS and which vary greatly as forest-influenced airmasses from burnt and unburnt regions are encountered. These data are reported in greater detail by Purvis et al. (2012).

The ozone photochemistry associated with alkyl nitrates ($\sum$ANs, $\sum RONO_2$) and peroxy nitrates ($\sum$PNs, $\sum RO_2NO_2$) is described in section 1. The Thermal Dissociation Laser Induced Fluorescence (TD-LIF) system (Dari-Salisburgo et al., 2008; Di Carlo et al., 2012) observed NO_2, $\sum$PNs, $\sum$ANs and NO_y on the BAe-146 aircraft during BORTAS (Table 2). Analysis of simultaneous observations of $\sum$ANs, CO, O_3 and NO_2 during BORTAS showed that $\sum$AN formation suppresses O_3 production at the rate of $\leq$10 O_x (= O_3+NO_2) per $\sum$ANs. In plumes where CO and CH_4 are the main precursor of O_x formation, we observe a productive rate of $>$100 O_x per $\sum$ANs. Ongoing analysis will improve the separation of pyrogenic plumes to understand the role of $\sum$ANs during

the evolution of forest fire plumes. BORTAS included several profiles from the ground to upper tro-
465 posphere and showed a factor of five increase of $\sum$PNs in airmasses affected by wildfire emissions compared to ambient air. Based on coincident measurements of NO_2 we found that approximatelty 40% of the initial NO_x emissions from the fires are converted within a few hour to PAN, in agreement with analysis of ARCTAS-B data (Alvarado et al., 2010).

Ozone photochemistry in boreal biomass burning plumes was evaluated using measurements of
470 NMHCs and NO_y species made from the BAe-146 with different instruments. The observed O_3 distribution in pyrogenic outflow, identified using tracers such as CO, and CH_3CN, during the campaign showed no distinguishable difference to the observed distribution in clean air. At the highest values of CO (>300 ppb) O_3 mixing ratios were observed in a relatively narrow range between approximately 40 and 60 ppb. Photochemical processes influencing the O_3 distribution in boreal
475 biomass burning plumes were evaluated through photochemical age calculations using ratios of different alkanes assuming a common sink of oxidation by OH (Parrish et al., 2007)) and comparison of the observed O_3 distribution relative to total alkyl nitrates and the surrogate species NO_z (= NO_y minus NO_x, the sum of NO_x oxidation products) (Olszyna et al., 1994; Rickard et al., 2002), representing the conversion of NO_x into O_3 (Parrington et al., 2013). Photochemical ages, calculated
480 relative to initial mixing ratios derived from research flight B626 over Northwestern Ontario, produced values of between 2–3 days aging for the strongest plumes (CO>300 ppb) encountered in the lower troposphere earlier in the campaign (i.e. flights B622-B624) and 6–7 days for plume air that was encountered at higher altitudes later in the campaign (i.e. flights B628-B630); Table 6 reports the range of photochemical ages of pyrogenic plumes for each flight. Graphical comparison
485 of the O_3 distribution to that of the alkyl nitrates and NO_z revealed clear 'L-shape' patterns with higher values of alkyl nitrates/NO_z at lower values of O_3, and lower values of alkyl nitrates/NO_z at higher O_3. The two branches of these 'L-shape' patterns revealed a clear distinction between measurements with different characteristics: 1) high measurements of alkyl nitrates/NO_z and lower O_3 were typically made at lower altitudes (below 5 km) with higher values of black carbon counts
490 (greater than 20) and at higher relative humidity (greater than 80%); and 2) low alkyl nitrates/NO_z and high O_3 measurements were typically made at higher altitudes, with lower black carbon (<20), and low relative humidity (<80%). Further comparison of the O_3 forming potential, calculated from the ratio of O_3:NO_z, to measured NO_x mixing ratios indicated that BORTAS measurements were made under different chemical regimes. Lower values of O_3 production efficiency (less that 150 ppb
495 O_3/ppb NO_z) show a larger range of NO_x mixing ratios (0.05-1.0 ppb) indicative of a VOC-limited regime, and higher values (greater than 150 ppb O_3/ppbNO_z) show a narrower range of NO_x mixing ratios (0.0-0.2 ppb) indicative of a NO_x-limited regime. This work is reported by Parrington et al. (2013).

Source attribution of observed variations in $PM_{2.5}$ at the DGS was achieved using a combination
500 of statistical data analysis and atmospheric transport modelling. During the BORTAS-B period 45

consecutive days of filter samples were collected at the DGS, the analysis from which was combined with continuous measurements of black carbon (BC) and organic carbon (OC) (Table 4). The US EPA Positive Matrix Factorization v3.0 (PMF) receptor model (Paatero and Trapper, 1994) was used to determine the source contribution of boreal forest fire aerosol to the total surface $PM_{2.5}$ mass concentration in Halifax (Song et al., 2001; Larson et al., 2004). The identification of the boreal forest fire source factor within PMF was characterized by the simultaneous increase in the chemical markers potassium and BC and corresponding decreases in other source markers, e.g. secondary ions, surficial material, sea salt, ship and vehicle emissions (C.-H. et al., 2008; Ward et al., 2012). The identified boreal forest fire source factor was also found to be coincident with FLEXPART and HYSPLIT back trajectories from known boreal forest fire source regions and with corresponding elevated surface CO concentrations predicted using the GEOS-Chem model. Measurements from the Raman LiDAR and from the BAe-146 that provided further evidence for boreal forest fire aerosol contributing to surface $PM_{2.5}$ mass concentration in Halifax (Gibson et al., 2012).

Describing the observed photochemistry using a hierarchy of chemical mechanisms, a core objective of BORTAS, allows us to investigate the uncertainties in our understanding O_3 production and loss within the biomass burning outflow and to quantify the resulting perturbation to tropospheric chemistry over the western boundary of the North Atlantic. Here, we used v3.2 of the MCM (http://mcm.leeds.ac.uk/MCM), a near-explicit chemical mechanism describing the detailed gas-phase degradation of a series of primary emitted VOCs (Saunders et al., 2003), which contains 143 primary emitted VOCs, 6,700 species involved in 17,000 reactions. We also used a reduced chemical mechanism, the "common representative intermediates" (CRM mechanism) (Jenkin et al., 2008), which is benchmarked against the more comprehensive MCM. The CRI mechanism provides an economical alternative to the MCM that can be applied to global 3-D CTMs such as GEOS-Chem whilst retaining much of the fidelity of the more detailed mechanism. The CRI mechanism contains a series of generic intermediate radicals and products (based on the O_3 creation potential for a given VOC) each of which is able to represent a larger set of species in the MCM. These generic intermediates mediate the breakdown of larger VOCs into smaller fragments, the chemistry of which is treated explicitly. The latest version of the CRI mechanism (v2) contains 442 species and 1191 reactions (7% of the full MCM). These mechanisms will be compared against the GEOS-Chem mechanism that is much less detailed than the CRI mechanism. We have used photochemical models that incorporate MCMv3.2 and CRIv2 mechanisms and constrained them with BORTAS aircraft observations to 1) investigate the chemistry controlling O_3 formation and loss and NO_y speciation along each BORTAS flight track, 2) evaluate the CRI mechanism, and subsequent reduced versions (Watson et al., 2008), and the GEOS-Chem mechanism, against the benchmark MCM, and 3) evaluate the initialization and speciation methodologies applied during the bottom-up model studies (Hays et al., 2002; Simpson et al., 2011). The majority of the calculations using the CRI mechanism reproduce the benchmark MCM calculations over 5–10 days, with most of the photochemical O_3

formed within the first 12–15 hours of daylight after emission, and capture most of the variation in the aircraft observations. This work is described by Young et al. (2012).

5 Concluding Remarks

The BORTAS-B experiment during 12th July–3rd August 2011 has delivered a large, diverse, and publicly available dataset that brings together aircraft, ground-based, balloon, and space-borne data associated with the pyrogenic emission and subsequent transport and photochemical aging of associated airmasses over Canada. The timing of the experiment reflects the climatological maximum of burning over this geographical region. Our choice to base the UK BAe-146-301 Atmospheric Research Aircraft at Halifax, Nova Scotia was because this region was one of the climatological loci of burning outflow over eastern Canada.

We have described the BORTAS experimental objectives and the methods and data we used to address them. We have also included brief descriptions of the Canadian ground station at Dalhousie University, which included a large suite of measurements to characterize the composition of pyrogenic material at ground level and to investigate trace gases and aerosols above the site, and the Pico Mountain Atmospheric Observatory in the Azores, located in the free troposphere days downwind of North American fires.

During the experiment, in order to help us determine our flight plans we used a combination of GEOS-5 forecast 3-D fields of CO, near-real time measurements of CO from the IASI satellite, and a range of meteorological products from Environment Canada, ECMWF and the UK Meteorological Office. We found the GEOS-5 forecast fields were generally reliable (without using any quantitative metric) in helping us laterally intercept both near-field and far-field pyrogenic plumes. We found pyrogenic plumes travelled in vertical filaments of the order of 100 m, even far downwind of any potential source.

The Northwestern Ontario fires, whilst devastating for local communities, provided BORTAS-B an unprecedented opportunity to sample near-field and far-field measurements from the same fires, allowing us to evaluate a variety of models based on our fundamental understanding of atmospheric photochemistry. The high-resolution/frequency measurements aboard the UK BAe-146 in particular provided a wealth of information about emissions, chemical aging of airmasses, and the subsequent transport of plumes. Some early results, described briefly in this paper, already reveal new insights about plume chemistry.

Synthesis and integration of a wide range of observations/modelling tools is required to look at the effect of biomass burning over a range of temporal and spatial scales. Preliminary analysis of coordinated measurements from space-borne, aircraft, and ground-based sensors and the GEOS-Chem global 3-D atmospheric chemistry transport model is encouraging with similar vertical structure associated with plumes. This level of coordination, while often non-trivial, provides invaluable val-

idation of the satellite data and confidence in our scaling up of aircraft measurements using models and global space-borne data.

Beyond the initial tranche of studies, described here, there is substantial science to be done with these data. In the short term, we want to understand how much error is introduced in, say, our understanding of O_3 production and loss within plumes by systematically simplifying the photochemistry. Within BORTAS-B we are developing a scheme that has been traceably reduced from the Master Chemical Mechanism (Saunders et al., 2003) moving towards the number of reactions that can be supported by a global 3-D chemistry transport model. Also in the short-term we want to understand how these data can improve our quantitative understanding to chemistry on the regional to hemispheric scale. This will be achieved using a data assimilation methodology (e.g., Parrington et al. (2012)) that can effectively extrapolate the detailed information collected during BORTAS-B to the larger domains. In the longer term putting BORTAS-B into context with all similar previous studies using, for example, a consistent modelling framework will result in additional insights into the underlying chemistry associated with the pyrogenic environment.

Acknowledgements. Airborne data were obtained using the BAe-146-301 Atmospheric Research Aircraft (ARA) operated by Directflight Ltd (DFL) and managed by the Facility for Airborne Atmospheric Measurements (FAAM), which is a joint entity of the Natural Environment Research Council (NERC) and the UK Meteorological Office. The BORTAS science team acknowledge the great efforts provided by the staff of FAAM, DFL, Avalon Aero Ltd and Captains Alan Foster and Charlie Whittaker and First Officer Ian Ramsay-Rae. We thank Environment Canada (EC) for meteorological forecasting support; R. Hoff (U. Maryland), and A. O'Neill (U. de Sherbrooke) for LiDAR and AOD measurements; G. Forbes, J. Davies, I. Beres, R. Mittermeier (EC), M. Osman (U. Western Ontario); A. Yamamoto (U. McGill), and L.-P. Beaudoin (Canadian Space Agency, CSA) for special ozonesonde launches; M. Bourqui (U. McGill) and H. He (EC) for trajectory forcasts; and most especially the many observers who obtained the ozonesonde measurements at the BORTAS sites. We also acknowledge Stephen Mobbs who agreed to release additional NCAS flight hours during BORTAS. This research was supported by the Natural Environment Research Council under grant number NE/F017391/1. PIP also acknowledges support from the Leverhulme Trust and the Nuffield Foundation. DM and JM acknowledge funding from the NERC National Centre for Earth Observation. Funding for the ozonesondes was provided by Environment Canada and the Green Horse Society (for Sable Island). The measurements at the Dalhousie Ground Station were supported by the Natural Sciences and Engineering Research Council of Canada. The Atmospheric Chemistry Experiment (ACE), also known as SCISAT, is a Canadian-led mission mainly supported by the Canadian Space Agency and the Natural Sciences and Engineering Research Council (NSERC) of Canada. Funding for the TAO measurements was provided by NSERC, CSA, and EC.

References

Alvarado, M. J., Logan, J. A., Mao, J., Apel, E., Riemer, D., Blake, D., Cohen, R. C., Min, K.-E., Perring, A. E., Browne, E. C., Wooldridge, P. J., Diskin, G. S., Sachse, G. W., Fuelberg, H., Sessions, W. R., Harrigan, D. L., Huey, G., Liao, J., Case-Hanks, A., Jimenez, J. L., Cubison, M. J., Vay, S. A., Weinheimer, A. J., Knapp, D. J., Montzka, D. D., Flocke, F. M., Pollack, I. B., Wennberg, P. O., Kurten, A., Crounse, J., Clair, J. M. S., Wisthaler, A., Mikoviny, T., Yantosca, R. M., Carouge, C. C., and Le Sager, P.: Nitrogen oxides and PAN in plumes from boreal fires during ARCTAS-B and their impact on ozone: an integrated analysis of aircraft and satellite observations, Atmospheric Chemistry and Physics, 10, 9739–9760, doi:10.5194/acp-10-9739-2010, http://www.atmos-chem-phys.net/10/9739/2010/, 2010.

Andreae, M. O. and Merlet, P.: Emission of trace gases and aerosols from biomass burning, Global Biogeochem. Cycles, 15, 955–966, doi: 10.1029/2000GB001382, 2001.

Atkinson, R. and Arey, J.: Atmospheric degradation of volatile organic compounds, Chem. Rev., 103, 4605–4638, 2003.

Beer, R., Glavich, T. A., and Rider, D. M.: Tropospheric emission spectrometer for the Earth Observing System's Aura satellite, Appl. Optics, 40, 2356–2367, 2001.

Bernath, P. F., McElroy, C. T., Abrams, M. C., Boone, C. D., Butler, M., Camy-Peyret, C., Carleer, M., Clerbaux, C., Coheur, P. F., Colin, R., DeCola, P., DeMaziere, M., Drummond, J. R., Dufour, D., Evans, W. F. J., Fast, H., Fussen, D., Gilbert, K., Jennings, D. E., Llewellyn, E. J., Lowe, R. P., Mahieu, E., McConnell, J. C., McHugh, M., McLeod, S. D., Michaud, R., Midwinter, C., Nassar, R., Nichitiu, F., Nowlan, C., Rinsland, C. P., Rochon, Y. J., Rowlands, N., Semeniuk, K., Simon, P., Skelton, R., Sloan, J. J., Soucy, M. A., Strong, K., Tremblay, P., Turnbull, D., Walker, K. A., Walkty, I., Wardle, D. A., Wehrle, V., Zander, R., and Zou, J.: Atmospheric Chemistry Experiment (ACE): Mission overview, Geophys. Res. Lett., 32, 2005.

Bitar, L., Duck, T. J., Kristiansen, N. I., Stohl, A., and Beaichamp, S.: Lidar observations of Kasatochi volcano aerosols in the troposphere and stratosphere, J. Geophys. Res., 115, doi:10.1029/2009JD013650, 2010.

Bourqui, M. S., Yamamoto, A., Tarasick, D., Moran, M. D., Beaudoin, L.-P., Beres, I., Davies, J., Elford, A., Hocking, W., Osman, M., and Wilkinson, R.: A new global real-time Lagrangian diagnostic system for stratosphere-troposphere exchange: evaluation during a balloon sonde campaign in eastern Canada, Atmospheric Chemistry and Physics, 12, 2661–2679, doi:10.5194/acp-12-2661-2012, http://www.atmos-chem-phys.net/12/2661/2012/, 2012.

C.-H., J., Evans, G. J., Dann, T., Graham, M., Herod, D., Dabek-Ziotorzynska, E., Mathieu, D., Ding, L., and Wang, D.: Influence of biomass burning on wintertime fine particulate matter: source contribution at a valley site in rural British Columbia, Atmos. Env., 42, 3684–3699, 2008.

Christian, T. J., Kleiss, B., Yokelson, R. J., Holzinger, R., Crutzen, P. J., Hao, W. M., Shirai, T., and Blake, D. R.: Comprehensive laboratory measurements of biomass-burning emissions: 2. First intercomparison of open-path FTIR, PTR-MS, and GC- MS/FID/ECD, J. Geophys. Res., 2004.

Clerbaux, C., Boynard, A., Clarisse, L., George, M., Hadji-Lazaro, J., Herbin, H., Hurtmans, D., Pommier, M., Razavi, A., Turquety, S., Wespes, C., and Coheur, P.-F.: Monitoring of atmospheric composition using the thermal infrared IASI/MetOp sounder, Atmospheric Chemistry and Physics, 9, 6041–6054, doi:10.5194/acp-9-6041-2009, http://www.atmos-chem-phys.net/9/6041/2009/, 2009.

Dacre, H. F., Grant, A. L. M., and Johnson, B. T.: Aircraft observations and model simulations of concentration

and particle size distribution in the Eyjafjallajökull volcanic ash cloud, Atmos. Chem. Phys., 12, 22 587–22 627, 2012.

Dari-Salisburgo, C., Carlo, P. D., Giammaria, F., Kajii, Y., and DAltorio, A.: Laser induced fluorescence instrument for NO_2 measurements: Observations at a central Italy background site, Atm. Env, 43, 970–977, 2008.

Di Carlo, P., Aruffo, E., Busilacchio, M., Giammaria, F., Dari-Salisburgo, C., Biancofiore, F., Visconti, G., Lee, J., Moller, S., Reeves, C. E., Bauguitte, S., Forster, G., Jones, R. L., and Ouyang, B.: Aircraft based four-channel thermal dissociation laser induced fluorescence instrument for simultaneous measurements of NO_2, total peroxy nitrate, total alkyl nitrate, and HNO_3, Atmospheric Measurement Techniques Discussions, 5, 8759–8787, doi:10.5194/amtd-5-8759-2012, http://www.atmos-meas-tech-discuss.net/5/8759/2012/, 2012.

Draxler, R. R.: HYSPLIT4 user's guide, Tech. Rep. NOAA Tech. Memo. ERL ARL-230, NOAA Air Resources Laboratory, Silver Spring, MD, 1999.

Drysdale, D.: An introduction to fire dynamics, John Wiley & Sons, 2008.

Fischer, H., Birk, M., Blom, C., Carli, B., Carlotti, M., von Clarmann, T., Delbouille, L., Dudhia, A., Ehhalt, D., Endemann, M., Flaud, J. M., Gessner, R., Kleinert, A., Koopman, R., Langen, J., López-Puertas, M., Mosner, P., Nett, H., Oelhaf, H., Perron, G., Remedios, J., Ridolfi, M., Stiller, G., and Zander, R.: MIPAS: an instrument for atmospheric and climate research, Atmospheric Chemistry and Physics, 8, 2151–2188, doi:10.5194/acp-8-2151-2008, http://www.atmos-chem-phys.net/8/2151/2008/, 2008.

Franklin, J. E., Griffin, D., Pierce, J. R., Drummond, J. R., Waugh, D., Palmer, P. I., Chisholm, L., Duck, T. J., Lesins, G., Walker, K. A., Hopper, J. T., Curry, K. R., Sakamoto, K. M., and O'Neill, N.: Remote sensing of trace gases and aerosols in biomass burning plumes over eastern Canada during the BORTAS field campaign, Atmos. Chem. Phys., 2012.

Fu, D., Walker, K. A., Sung, K., Boone, C. D., Soucy, M.-A., and Bernath, P. F.: The portable atmospheric research interferometric spectrometer for the infrared, PARIS-IR, J. Quant. Spectro. and Rad. Trans., 103, 362–370, 2007.

George, M., Clerbaux, C., Hurtmans, D., Turquety, S., Coheur, P.-F., Pommier, M., Hadji-Lazaro, J., Edwards, D. P., Worden, H., Luo, M., Rinsland, C., and McMillan, W.: Carbon monoxide distributions from the IASI/METOP mission: evaluation with other space-borne remote sensors, Atmospheric Chemistry and Physics, 9, 8317–8330, doi:10.5194/acp-9-8317-2009, http://www.atmos-chem-phys.net/9/8317/2009/, 2009.

Gerbig, C., Schmitgen, S., Kley, D., Volz-Thoms, A., Dewey, K., and Haaks, D.: An improved fast-response vacuum-UV resonance fluorescence CO instrument, J. Geophys. Res., 104, 1699–1704, 1999.

Gibson, M. D., Heal, M. R., Bachse, D. H., Hursthouse, A. S., Beverland, I. J., Craig, S. E., Clak, C. F., Jackson, M. H., Guernsey, J. R., and Jones, C.: Using Mass Reconstruction along a Four-Site Transect as a method to interpret PM10 in West-Central Scotland, J. Air and Waste Management Assoc., 59, 1429–1436, 2009.

Gibson, M. D., Kuchta, J., Chisholm, L., Duck, T., Hopper, J., Beauchamp, S., King, G., Waugh, D., Pierce, J., Wheeler, A., Li, Z., and Palmer, P. I.: Receptor modelling of surface $PM_{2.5}$ in Halifax, Nova Scotia, Canada during the 2011 BORTAS aircraft campaign, In Prep., 2012.

Griffin, D., Franklin, J., Parrington, M., Whaley, C., Hopper, J., Lesins, G., Tereszchuk, K., Walker, K. A., Drummond, J. R., Palmer, P. I., Strong, K., Duck, T. J., Abboud, I., Dan, L., O'Neill, N., Clerbaux, C.,

Coheur, P., Bernath, P. F., Hyer, E., and Kliever, J.: Investigation of CO, C_2H_6 and aerosols over eastern Canada during BORTAS 2011 using ground-based and satellite-based observations and model simulations, Atmos. Chem. Phys., 2012.

Hays, M. D., Geron, C. D., Linna, K. J., Smith, N. D., and Schauer, J. J.: Speciation of Gas-Phase and Fine Particle Emissions from Burning of Foliar Fuels, Environmental Science & Technology, 36, 2281–2295, doi:10.1021/es0111683, http://pubs.acs.org/doi/abs/10.1021/es0111683, 2002.

Holben, B. N., Eck, T. F., Slutsker, I., Tanre, D., Buis, J. P., Setzer, A., Vermote, E., Reagan, J. A., Kaufman, Y., Nakajima, T., Lavenu, F., Jankowiak, I., and Smirnov, S.: AERONET - A federated instrument network and data archive for aerosol characterization, Rem. Sens. Environ., 66, 1998.

Honrath, R. E., Owen, R. C., Martin, M. V., Reid, J. S., Lapina, K., Fialho, P., Dziobak, M. P., Kleissl, J., and Westphal, D. L.: Regional and hemispheric impacts of anthropogenic and biomass burning emissions on summertime CO and O3 in the North Atlantic lower free troposphere, J. Geophys. Res., 2004.

Honrath, R. E., Helmig, D., Owen, R. C., Parrish, D. D., and Tanner, D. M.: Nonmethane hydrocarbons at Pico Mountain, Azores: 2. Event-specific analyses of the impacts of mixing and photochemistry on hydrocarbon ratios, J. Geophys. Res., 113, doi:10.1029/2008JD009832, 2008.

Hopkins, J. R., Read, K. A., and Lewis, A. C.: Two Column Method For Long-term Monitoring Of Non-Methane Hydrocarbons (NMHCs) and Oxygenated Volatile Organic Compounds, J. Env. Monitoring, 5, 8–13, 2003.

Illingworth, S. M., Remedios, J. J., Boesch, H., Moore, D. P., Sembhi, H., Dudhia, A., and Walker, J. C.: ULIRS, an optimal estimation retrieval scheme for carbon monoxide using IASI spectral radiances: sensitivity analysis, error budget and simulations, Atmospheric Measurement Techniques, 4, 269–288, doi:10.5194/amt-4-269-2011, http://www.atmos-meas-tech.net/4/269/2011/, 2011.

Jacob, D. J., Crawford, J. H., Maring, H., Clarke, A. D., Dibb, J. E., Emmons, L. K., Ferrare, R. A., Hostetler, C. A., Russell, P. B., Singh, H. B., Thompson, A. M., Shaw, G. E., McCauley, E., Pederson, J. R., and Fisher, J. A.: The Arctic Research of the Composition of the Troposphere from Aircraft and Satellites (ARCTAS) mission: design, execution, and first results, Atmos. Chem. Phys., 10, 5191–5212, 2010.

Jaffe, D. A. and Wigder, N. L.: Ozone production from wildfires: a critical review, Atmos. Env., 51, 1–10, 2012.

Jayne, J. T., Heard, D. C., Zhang, X. F., Davidovits, P., Smith, K. A., Kolb, C. E., and Worsnop, D. R.: Development of an aerosol mass spectrometer for size and composition analysis of submicron particles, Aerosol Sci. Technol., 33, 49–70, 2000.

Jenkin, M., Watson, L., Utembe, S., and Shallcross, D.: A Common Representative Intermediates (CRI) mechanism for VOC degradation. Part 1: Gas phase mechanism development, Atmospheric Environment, 42, 7185 – 7195, doi:10.1016/j.atmosenv.2008.07.028, http://www.sciencedirect.com/science/article/pii/S1352231008006742, 2008.

Junkermann, W., Platt, U., and Volz-Thomas, A.: A photoelectric detector for the measurement of photolysis frequencies of ozone and other atmospheric molecules, J. Atmos. Chem., 8, 203–227, 1989.

Keil, C. and Craig, G. C.: A displacement and amplitude score employing an optical flow technique, Weather and Forecasting, 24, 1297–1308, doi:10.1175/2009WAF2222247.1, 2009.

Kulawik, S. S., Bowman, K. W., Luo, M., Rodgers, C. D., and Jourdain, L.: Impact of nonlinearity on changing

the a priori of trace gas profile estimates from the Tropospheric Emission Spectrometer (TES), Atmos. Chem. Phys., 2008.

Larson, T., Gould, T., Simpson, C., Liu, L. J., Claiborn, C., and Lewtas, J.: Source apportionment of indoor, outdoor, and personal PM2.5 in Seattle, Washington, using positive matrix factorization, J. Air Waste Manag. Assoc., 54, 1175–1187, 2004.

Lee, J. D., Moller, D. J., Read, K. A., Lewis, A. C., Mendes, L., and Carpenter, L. J.: Year-round measurements of nitrogen oxides and ozone in the tropical North Atlantic marine boundary laer, J. Geophys. Res., 114, doi:10.1029/2009JD011878, 2009.

Leiterer, U., Naebert, A., Naebert, T., and Alekseeva, G.: A new star photometer developed for spectral aerosol optical thickness measurements in Lindenberg, Contrib. Atmos. Phys., 68, 133–141, 1995.

Lenschow, D. H.: Probing the atmospheric boundary layer, chap. Aircraft measurements in the boundary layer, pp. 39–55, Amer. Meteor. Soc., 1986.

Lewis, A. C., Evans, M. J., Methven, J., Watson, N., Lee, J. D., Hopkins, J. R., Purvis, R. M., Arnold, S. R., McQuaid, J. B., Whalley, L. K., Pilling, M. J., Heard, D. E., Monks, P. S., Parker, A. E., Reeves, C. E., Oram, D. E., Mills, G., Bandy, B. J., Stewart, D., Coe, H., Williams, P., and Crosier, J.: Chemical composition observed over the mid-Atlantic and the detection of pollution signatures far from source regions, J. Geophys. Res., 112, doi:10.1029/2006JD007584, 2007.

Lewis, A. C., Evans, M. J., Hopkins, J. R., Punjabi, S., Read, K. A., Andrews, S. J., Moller, S. J., Carpenter, L. J., Lee, J. D., Rickard, A., Palmer, P. I., and Parrington, M.: The influence of biomass burning on the global distribution of selected non-methane organic compounds, Atmos. Chem. Phys. Discuss, 2012.

Marple, V. A., Rubow, K. L., and Behm, S. M.: A Microorifice Uniform Deposit Impactor (MOUDI): Description, Calibration, and Use, Aerosol Science and Technology, 14, 434–446, doi:10.1080/02786829108959504, http://www.tandfonline.com/doi/abs/10.1080/02786829108959504, 1991.

Matthiesen, S., Palmer, P. I., and Parrington, M.: Development of a 3-dimensional quality forecast measure for plume forecasts, Atmos. Chem. Phys., 2012.

McConnell, C. L., Formenti, P., Highwood, E. J., and Harrison, M. A. J.: Using aircraft measurements to determine the refractive index of Saharan dust during the DODO Experiments, Atmospheric Chemistry and Physics, 10, 3081–3098, doi:10.5194/acp-10-3081-2010, http://www.atmos-chem-phys.net/10/3081/2010/, 2010.

Moore, D. P. and Remedios, J. J.: Seasonality of Peroxyacetyl nitrate (PAN) in the upper troposphere and lower stratosphere using the MIPAS-E instrument, Atmospheric Chemistry and Physics, 10, 6117–6128, doi:10.5194/acp-10-6117-2010, http://www.atmos-chem-phys.net/10/6117/2010/, 2010.

Moore, D. P., Remedios, J. J., and Waterfall, A. M.: Global distributions of acetone in the upper troposphere from MIPAS spectra, Atmospheric Chemistry and Physics, 12, 757–768, doi:10.5194/acp-12-757-2012, http://www.atmos-chem-phys.net/12/757/2012/, 2012.

Mota, B. W., Pereira, J. M. C., Oom, D., Vasconcelos, M. J. P., and Schultz, M.: Screening the ESA ATSR-2 World Fire Atlas (19972002), Atmospheric Chemistry and Physics, 6, 1409–1424, doi:10.5194/acp-6-1409-2006, http://www.atmos-chem-phys.net/6/1409/2006/, 2006.

Mu, M., Randerson, J. T., van der Werf, G. R., Giglio, L., Kasibhatla, P., Morton, D., Collatz, G. J., DeFries, R. S., Hyer, E. J., Prins, E. M., Griffiths, D. W. T., Wunch, D., Toon, G. C., Sherlock, V., and Wennberg, P. O.:

Daily and 3-hourly variability in global fire emissions and consequences for atmospheric model predictions of carbon monoxide, J. Geophys. Res., 116, doi:10.1029/2011JD016245, 2011.

Murphy, J. G., Oram, D. E., and Reeves, C. E.: Measurements of volatile organic compounds over West Africa, Atmos. Chem. Phys., 10, 5281–5294, 2010.

Ng, N. L., Herndon, S. C., Trimborn, A., Canagaratna, M. R., Croteau, P., Onasch, T. B., Sueper, D., Worsnop, D. R., Zhang, Q., Sun, Y. L., and Jayne, J. T.: An Aerosol Chemical Speciation Monitor (ACSM) for routine monitoring of the composition and mass concentrations of ambient aerosol, Aerosol Science and Technology, 45, 770–784, http://dx.doi.org/10.1080/02786826.2011.560211, 2011.

Olivier, J. G. J. and Berdowski, J. J. M.: The Climate System, chap. Global emissions sources and sinks, A.A. Balkema Publishers/Swets & Zeitlinger Publishers, 2001.

Olszyna, K. J., Bailey, E. M., Simonaitis, R., and Meagher, J. F.: O_3 and NO_y relationships at a rural site, J. Geophys. Res., 99, 14,557–14,563, 1994.

O'Shea, S. J., Bauguitte, S. J.-B., Gallagher, M. W., Lowry, D., and Percival, C. J.: Development of a cavity enhanced absorption spectrometer for airborne measurements of CH_4 and CO_2, Atmos. Meas. Tech., 2012.

Ott, L., Pawson, S., and Bacmeister, J.: An analysis of the impact of convective parameter sensitivity on simulated global atmospheric CO distributions, J. Geophys. Res., 116, doi: 10.1029/2011JD016077, 2011.

Paatero, P. and Trapper, U.: Positive matrix factorization: a non-negative factor model with optimal utilization of error estimates of data values, Environmetrics, 5, 111–126, 1994.

Parker, R. J., Remedios, J. J., Moore, D. P., and Kanawade, V. P.: Acetylene C_2H_2 retrievals from MIPAS data and regions of enhanced upper tropospheric concentrations in August 2003, Atmospheric Chemistry and Physics Discussions, 10, 29 735–29 771, doi:10.5194/acpd-10-29735-2010, http://www.atmos-chem-phys-discuss.net/10/29735/2010/, 2010.

Parrington, M., Palmer, P. I., Henze, D. K., Tarasick, D. W., Hyer, E. J., Owen, R. C., Helmig, D., Clerbaux, C., Bowman, K. W., Deeter, M. N., Barratt, E. M., Coheur, P.-F., Hurtmans, D., Jiang, Z., George, M., and Worden, J. R.: The influence of boreal biomass burning emissions on the distribution of tropospheric ozone over North America and the North Atlantic during 2010, Atmospheric Chemistry and Physics, 12, 2077–2098, doi:10.5194/acp-12-2077-2012, http://www.atmos-chem-phys.net/12/2077/2012/, 2012.

Parrington, M., Palmer, P. I., and et al: Aircraft observations of ozone photochemistry in the outflow from boreal biomass burning, Atmos. Chem. Phys. Discuss., 2013.

Parrish, D. D., Stohl, A., Forster, C., Atlas, E. L., Blake, D. R., Goldan, P. D., Kuster, W. C., and de Gouw, J. A.: Effects of mixing on evolution of hydrocarbon ratios in the troposphere, J. Geophys. Res., 112, 10.1029/2006JD007583, 2007.

Petersen, G. N. and Renfrew, I. A.: Aircraft-based observations of air-sea fluxes over Denmark Strait and the Irminger Sea during high wind speed conditions, Q. J. R. Meteorol. Soc., 135, 2030–2045, 2009.

Purvis, R. M., Lews, A. C., Hopkins, J. R., Andrews, S., and Minaean, J.: Functionalized aromatic compounds within middle troposphere boreal biomass burning plumes, In prep., 2012.

Real, E., Law, K. S., Weinzierl, B., Fiebig, M., Petzold, A., Wild, O., Methven, J., Arnold, S., Stohl, A., Huntrieser, H., Roiger, A., Schlager, H., Stewart, D., Avery, M., Sachse, G., Browell, E., Ferrare, R., and Blake, D.: Processes influencing ozone levels in Alaskan forest fire plumes during long-range transport over the North Atlantic,, J. Geophys. Res., 112, doi:10.1029/2006JD007576, 2007.

Reid, J. S., Hyer, E. J., Prins, E. M., Westphal, D. L., Zhang, J., Wang, J., Christopher, S. A., Curtis, C. A., Schmidt, C. C., Eleuterio, D. P., Richardson, K. A., and Hoffman, J. P.: Global monitoring and forecasting of biomass burning smoke: Description of and lessons from the Fire Locating and Modeling of Burning Emissions (FLAMBE) program, IEEE J. Selected Topics in Appl Earth Obs. and Remote Sensing, 2, 144–162, 2009.

Reidmiller, D. R., Jaffe, D. A., Fischer, E. V., and Finley, B.: Nitrogen oxides in the boundary layer and free troposphere at the Mt. Bachelor Observatory, Atmospheric Chemistry and Physics, 10, 6043–6062, doi: 10.5194/acp-10-6043-2010, http://www.atmos-chem-phys.net/10/6043/2010/, 2010.

Rickard, A. R., Salisbury, G., Monks, P. S., Lewis, A. C., Baugitte, S., Bandy, B. J., Clemitshaw, K. C., and Penkett, S. A.: Comparison of measured ozone production efficiencies in the marine boundary layer at two European coastal sites under different pollution regimes, J. Atmos. Chem., 43, 107–134, 2002.

Rienecker, M. M., Suarez, M. J., Todling, R., Bacmeister, J., Takacs, L., Liu, H.-C., Gu, W., Sienkiewicz, M., Koster, R. D., Gelaro, I., and Nielsen, J. E.: The GEOS-5 Data Assimilation System - Documentation of Versions 5.0.1, 5.1.0, and 5.2.0, Tech. rep., NASA Goddard, 2008.

Rodgers, C. D. and Connor, B. J.: Intercomparison of remote sounding instruments, J. Geophys. Res., 108, doi:10.1029/2002JD002299, 2003.

Ryerson, T. B., Trainer, M., Holloway, J. S., Parrish, D. D., Huey, L. G., Sueper, D. T., Frost, G. J., Donnelley, S. G., Schauffer, S., Atlas, E. L., Kuster, W. C., Goldan, P. D., Hübler, G., and Meagher, J. F.: Observations of Ozone Formation in Power Plant Plumes and Implications for Ozone Control Strategies, Science, 292, 719–723, doi:10.1126/science.1058113, 2001.

Saunders, S. M., Jenkin, M. E., Derwent, R. G., and Pilling, M. J.: Protocol for the development of the Master Chemical Mechanism MCM v3 (Part A): tropospheric degradation of nonaromatic volatile organic compounds, ACP, 3, 161–180, doi:10.5194/acp-3-161-2003, 2003.

Simpson, I. J., Akagi, S. K., Barletta, B., Blake, N. J., Choi, Y., Dirkin, G. S., Fried, A., Fuelberg, H. E., Meinardi, S., Rowland, F. S., Vay, S. A., Weinheimer, A. J., Wennberg, P. O., Wiebring, P., Wisthaler, A., Yang, M., Yokelson, R. J., and Blake, D. R.: Boreal forest fire emissions in fresh Canadian smoke plumes: C_1-C_10 volatile organic compounds (VOCs), CO_2, CO, NO_2, NO, HCN and CH_3CN, Atm. Chem. Phys., 2011.

Song, X.-H., Polissar, A. V., and Hopke, P. K.: Sources of fine particle composition in the northeastern US, Atmos. Env., 35, 5277–5286, 2001.

Strawbridge, K. B.: Developing a portable, autonomous aerosol backscatter lidar for network or remote operations, Atmospheric Measurement Techniques Discussions, 5, 8609–8652, doi:10.5194/amtd-5-8609-2012, http://www.atmos-meas-tech-discuss.net/5/8609/2012/, 2012.

Ström, J., Busen, R., Quante, M., Guillemet, B., Brown, P. R. A., and Heintzenberg, J.: Pre-EUCREX intercomparison of airborne humidity measuring instruments, J. Atmos. Tech., 11, 1994.

Tereszchuk, K. A., González Abad, G., Clerbaux, C., Hurtmans, D., Coheur, P.-F., and Bernath, P. F.: ACE-FTS measurements of trace species in the characterization of biomass burning plumes, Atmospheric Chemistry and Physics, 11, 12 169–12 179, doi:10.5194/acp-11-12169-2011, http://www.atmos-chem-phys.net/11/12169/2011/, 2011.

Tereszchuk, K. A., González, A. G., Clerbaux, C., Hadji-Lazaro, J., Hurtmans, D., Coheur, P.-F., and Bernath,

P. F.: ACE-FTS Observations of Pyrogenic Trace Species in Boreal Biomass Burning Plumes During BORTAS, Atmos. Chem. Phys., 2012.

Verma, S., Worden, J., Pierce, B., Jones, D. B. A., Al-Saadi, J., Boersma, F., Bowman, K., Eldering, A., Fisher, B., Jourdain, L., Kulawik, S., and Worden, H.: Ozone production in boreal fire smoke plumes using observation from the Tropospheric Emission Spectrometer and the Ozone Monitoring Instrument, J. Geophys. Res., 114, doi:10.1029/2008JD010108, 2009.

Volz-Thomas, A., Lerner, A., Pätz, H.-W., Schultz, M., McKenna, D. S., Schmitt, R., Madronich, S., and Röth, E. P.: Airborne measurements of the photolysis frequency of NO_2, J. Geophys. Res., 101, 18,613–18,627, 1996.

Ward, T., Trost, B., Conner, J., Flanagan, J., and Jayanty, R. K. M.: Source apportionment of PM2.5 in a subarctic airshed, Fairbanks, Alaska, Aerosol and Air Quality Research, 12, 536–543, 2012.

Watson, L., Shallcross, D., Utembe, S., and Jenkin, M.: A Common Representative Intermediates (CRI) mechanism for VOC degradation. Part 2: Gas phase mechanism reduction, Atmospheric Environment, 42, 7196 – 7204, doi:10.1016/j.atmosenv.2008.07.034, http://www.sciencedirect.com/science/article/pii/S1352231008006845, 2008.

Whalley, L. K., Lewis, A. C., McQuaid, J. B., Purvis, R. M., Lee, J. D., Stemmler, K., Zellweger, C., and Ridgeon, P.: Nonmethane Hydrocarbons and PAN at The Jungfraujoch High Altitude Station: A Test Of Chromatography Instruments Designed For Use On Research Aircraft., J. Env. Monitoring, 6, 234–241, 2004.

Wiacek, A., Taylor, J. R., Strong, K., Saari, R., Kerzenmacher, T. E., Jones, N. B., and Griffith, D. W. T.: Ground-Based Solar Absorption FTIR Spectroscopy: Characterization of Retrievals and First Results from a Novel Optical Design Instrument at a New NDACC Complementary Station, Journal of Atmospheric and Oceanic Technology, 24, 432, doi:10.1175/JTECH1962.1, 2007.

Wilson, K. L. and Birks, J. W.: Mechanism and elimination of a water vapor interferences in the measurement of ozone by UV absorbance, Environ. Sci. Technol., 40, 6361–6367, 2006.

Yokelson, R. J., Christian, T. J., Karl, T. G., and Guenther, A.: The tropical forest and fire emissions experiment: laboratory fire measurements and synthesis of campaign data, Atmos. Chem. Phys., 2008.

Young, J., Rickard, A. R., Jenkin, M. E., Parrington, D. S. M., Palmer, P. I., and et al: Net Ozone Production During the Chemical Evolution of Biomass Burning Plumes: Evaluation of a Hierarchy of Chemical Mechanisms, Atmos. Chem. Phys., 2012.

Table 1: Synoptic meteorology and associated with BORTAS flights over Canada.

Flight #, data	Sortie description	Synoptic Meteorology
B618, 12th July, 2011	Outbound transit 1: Cranfield, UK to Horta, Azores	
B618, 13th July, 2011	Outbound transit 2: Horta, Azores to St John's, NL	
B619, 13th July, 2011	Outbound transit 2: St John's, NL to Halifax, NS	
B620, 15th July, 2011	Halifax, NS-Quebec, NS-Halifax, NS	Low from surface to 500 hPa S of Sable Island. Weak ridge lowest levels over northern Gulf and southern Labrador. (Fig. 3a). Cloud over NS and Prince Edward Island otherwise clear.
B621a, 18th July, 2011	Halifax, NS-Goose Bay, NL	Weak short wave trough crossing Maritime Canada, cold front crossing Nova
B621b, 18th July, 2011	Goose Bay, NL - Halifax, NS	Scotia. Weak ridge building into S Labrador. (Fig. 3b). Cloud and precip over Nfld. Showers inland from the N shore of Gulf. Clearing skies for the return flight.
B622, 20th July 2011	Halifax, NS - Quebec City, QC	Low from surface to 500 hPa S Ungava Bay. Surface low and frontal wave moving E from mouth of St Lawrence. (Fig. 3c) Flight in warm sector skies mainly clear.
B623, 20th July, 2011	Quebec City, QC - Halifax	Low from surface to 500 hPa S Ungava Bay. Surface low and frontal wave just N of Anticosti Island and cold front west. (Fig. 3c). Showers and thundershowers along and in advance of front. Aircraft may have encountered showers over PEI.
B624, 21st July, 2011	Halifax, NS, - St John's, NL - Halifax, NS	Low from surface to 500 hPa over extreme N Labrador. Cold front from NB to S of NF. Weak low crossing NB late day. (Fig. 3d). Cloud moved into flight zone from the west. Precipitation for return flight from S of NF to Halifax.
B625, 24th July, 2011	Halifax, NS region	Low from surface to 500 hPa southern Davis Strait with trough to deepening low over NF moving east. (Fig. 3e). Cold front east of NF. Flight path in clear skies.
B626, 26th July, 2011	Halifax, NS - Thunder Bay, ON	Low from surface to 500 hPa over extreme S QC. Ridge surface and aloft over NW ON. (Fig. 3f). Flight in clouds westbound over S QC. Showers likely below flight level. Clear skies in ON.
B626, 26th July, 2011	Thunder Bay, ON, region	As above for flight B626 (Fig. 3f). Clear skies with convective clouds over NW ON. Some showers late in flight period.
B627, 27th July, 2011	Thunder Bay ON - Goose Bay, NL	Weak ridging over Ontario all levels and weak trough Labrador to Maritimes. (Fig. 3g). Cloud moving into western Ontario. Clear over E ON and W QC. Cumulus over central QC and Labrador.
B628a, 28th July, 2011	Goose Bay, NL, region	Weak ridge surface through to 500 hPa central Labrador to NB. (Fig. 3h). Mostly clear for flight route.
B628b, 28th July, 2011	Goose Bay, NL - Halifax, NS	Cumulus and towering cumulus over higher terrain southern Labrador.
B629, 31st July, 2011	Halifax, NS region	Trough from surface through to 500 hPa along Labrador coast to low centre off south coast NF. Cooler airmass over region. Weak ridge building over NB to W Labrador. (Fig. 3i). Generally clear skies for flight route and level.
B630, 31st July, 2011	Halifax, NS region	As above for Flight B629 (Fig. 3i).
B631, 2nd August, 2011	Halifax, NS to Horta, Azores	Return transit leg 1.
B631, 3rd August, 2011	Horta, Azores to Cranfield, UK	Return transit leg 2.

Table 2: BAe-146 payload during BORTAS.

Species/ parameter	Method	Averaging time	Precision/ accuracy	Reference/ affiliation
Position, winds, u, v, w	INS, GPS, 5-port turbulence probe	0.1 s	$0.01\Delta P/P_s$	FAAM, Petersen and Renfrew (2009)
Relative humidity	Hygrometer, General Eastern 1011b	4 Hz	$\pm$0.5–$\pm$3 K dependent on dew point and ambient conditions	FAAM, Ström et al. (1994)
Temperature	Rosemount Aerospace Ltd sensor 102 AL	32 Hz	$\pm$0.3 K	FAAM¡ Lenschow (1986)
CO	VUV resonance/fluorescence	1 s	1 ppb, 3%	FAAM, Gerbig et al. (1999).
CO_2, CH_4	Cavity enhanced absorption spectrometer	1 sec	At 1 Hz: 2.5 ppb for CH_4 and 0.5 ppm for CO_2	O'Shea et al. (2012), FAAM
O_3	UV absorption	3 Hz	1 ppb, $\pm$5%	FAAM, Wilson and Birks (2006)
HCN, HCOOH, N_2O_5	Chemical Ionisation Mass Spectrometer (CIMS)		26 ppt	U. Manchester
NO_2, $\sum RO_2NO_2$, $\sum RONO_2$, NO_y	Light Induced Fluorescence (LIF)	10 Hz	10%, 22%, 34%, and 46% for NO_2, $\sum PNs$, $\sum ANs$, and NO_y, respectively	Dari-Salisburgo et al. (2008) CETEMPS, Department of Physical and Chemical Sciences, University of L'Aquila, Italy
C_5–C_{12} VOCs	GC-MS	180 s	Species dependent typically 10 ppt (20%)	Purvis et al. (2012) U. York
C_2–C_7 NMHCs, acetone CH_3OH	WAS-GC	30 s fill time	Species dependent typically 1–5 ppt (5%)	Hopkins et al. (2003) U. York
CH_3CN, C_3H_6O, C_5H_8, MVK+MACR, C_4H_8O, C_6H_6, C_7H_8, $C_{10}H_{16}$	PTR-MS	1 s	37, 95, 120, 59, 61, 45, 109, 148 ppt, respectively. Mean of the precision estimates over all BORTAS flights.	Murphy et al. (2010)
NO, NO_2	Chemiluminescence, single-channel Air Quality Design Inc	10 s	10 ppt	FAAM, Lee et al. (2009); Reidmiller et al. (2010)
PAN	Dual column GC-ECD	90 s	3%, 10%	Whalley et al. (2004)
Non-refractory aerosol composition, 40–700 nm vacuum aerodynamics diameter	AMS	LOD[1]: 3ng/m^3 for nitrate and sulphate; 25ng/m^3 for organics; and 30ng/m^3 for ammonium. Precisions same as LOD. Accuracy: 20%.	15-150 ng/m^3	Jayne et al. (2000)
Refractory black carbon, 70–520 nm	SP2	Accuracy 20%, precision 5% at 5 s average		
jNO_2, jO^1D	Fixed bandwidth radiometry, 0.3–3.0μm	1 Hz	5.5%	Junkermann et al. (1989); Volz-Thomas et al. (1996) McConnell et al. (2010)

s

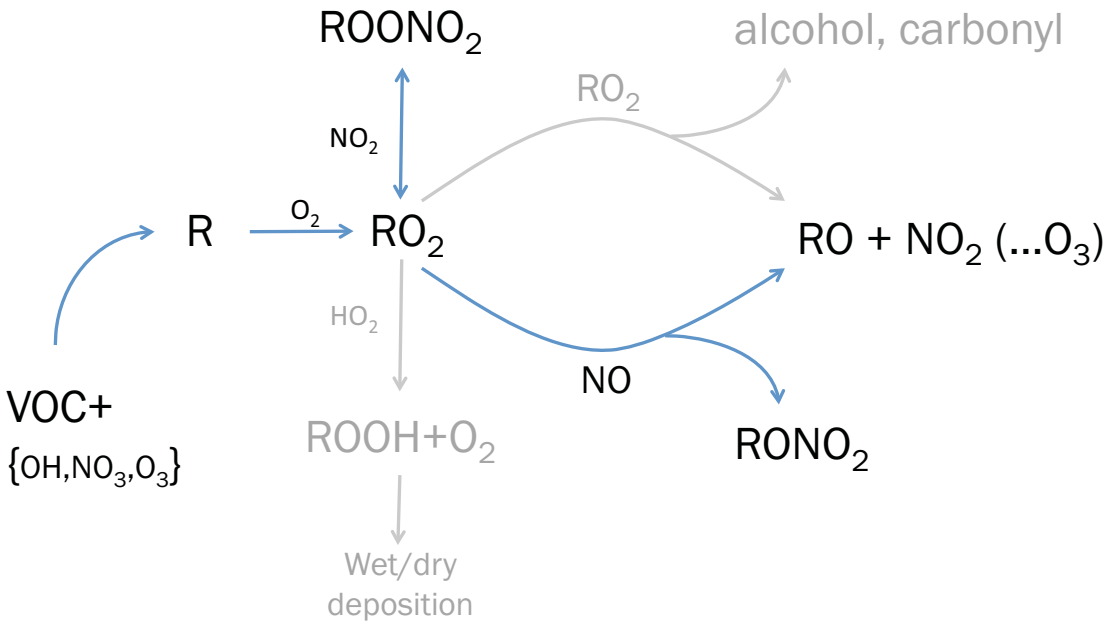

Fig. 1: A schematic of the atmospheric chemical system studied within BORTAS (Atkinson and Arey, 2003)

Table 3: Environment Canada ozonesonde launch sites during BORTAS A (2010) and B (2011).

Site	BORTAS-A launches[1]	BORTAS-B launches[2]
Alert, Nanavut (82°N, 62°W)	1	1
Bratt's Lake, Saskatchewan (50°N, 105°W)	18	20
Churchill, Manitoba (59°N, 94°W)	1	-
Egbert, Ontario (44°N, 80°W)	16	15
Eureka, Nunavut (80°N, 86°W)	2	2
Goose Bay, Newfoundland (53°N, 60°W)	20	20
Kelowna, British Columbia (50°N, 119°W)	2	2
Montreal, Quebec (45°N, 73°W)	19	-
Resolute, Nunavut (75°N, 95°W)	2	1
Sable Island, Nova Scotia (44°N, 60°W)	19	19
Stony Plain (Edmonton), Alberta (54°N, 114°W)	2	2
Walsingham, Ontario (43°N, 81°W)	14	-
Yarmouth, Nova Scotia (44°N, 66°W)	19	20

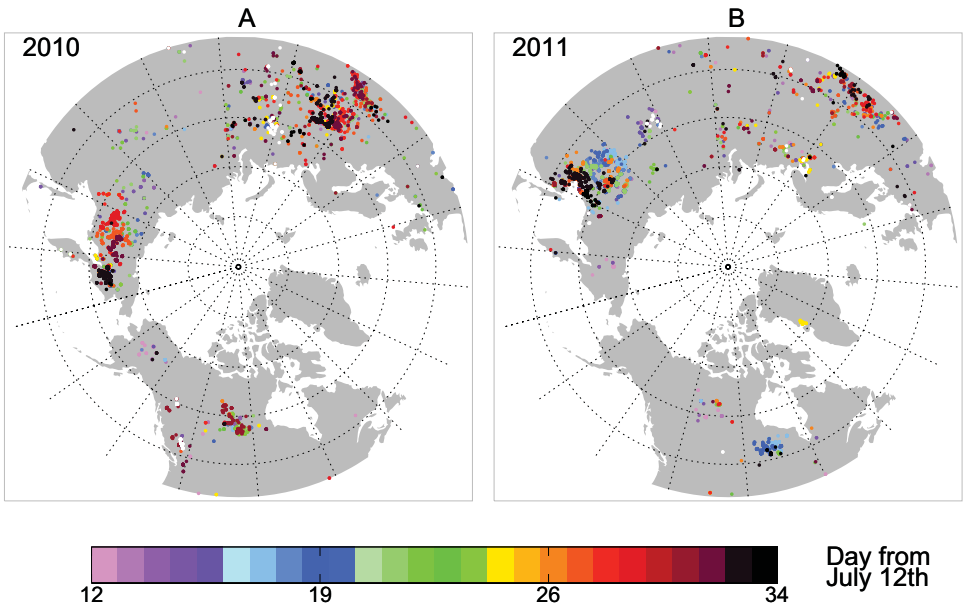

Fig. 2: Time and location of active fires during 12th July–3rd August 2010 (A) and 2011 (B), informed by the ATSR radiance measurements (Mota et al., 2006). The colour denotes the day from 12th July. ATSR firecount data are from ATSR-WFA, from the Data User Element of the European Space Agency.

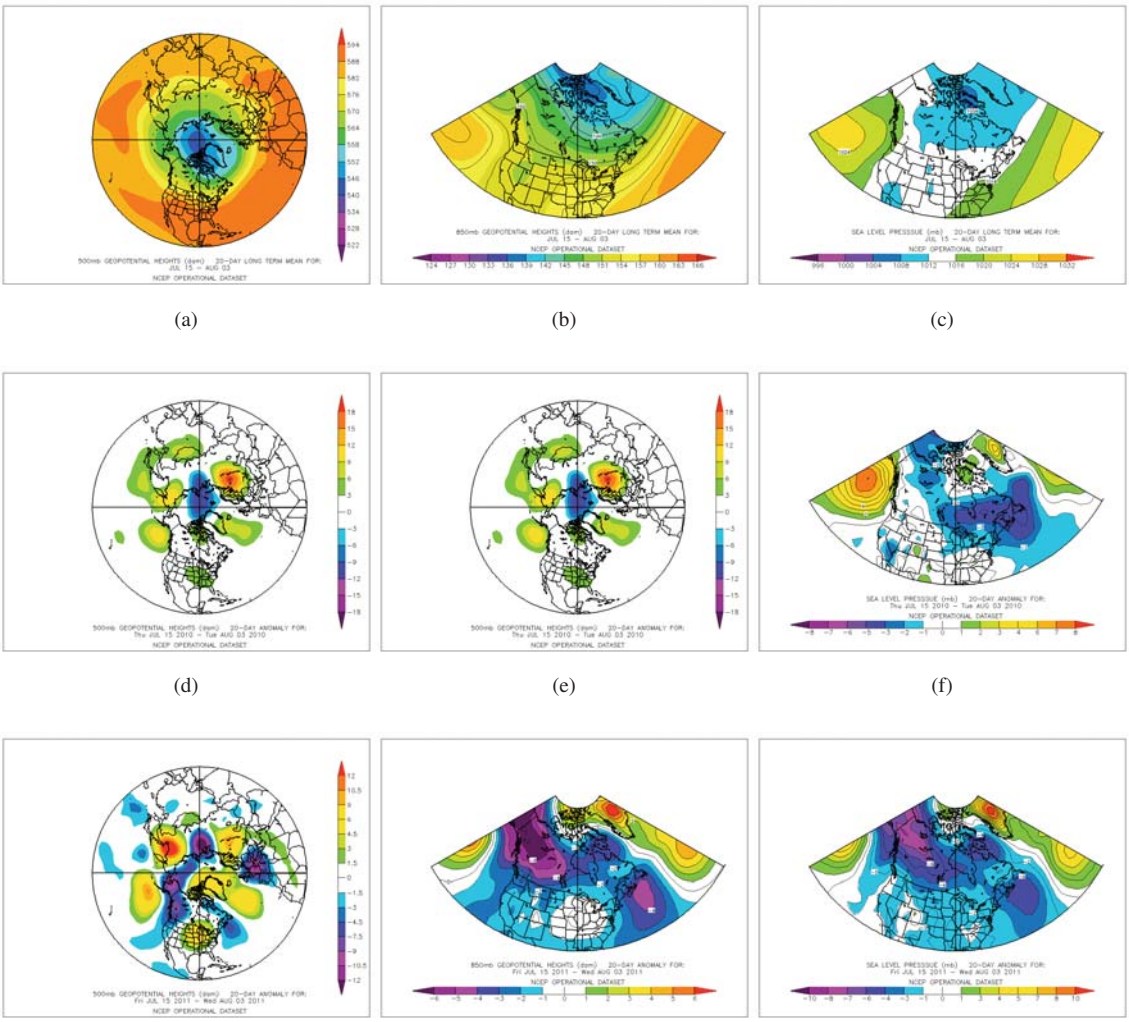

(a) (b) (c)

(d) (e) (f)

(g) (h) (i)

Fig. 3: Climatological mean 500 hPa (a) and 850 hPa (b) geopotential heights (expressed in decametres, dam), and sea level pressure (mb, c) for 15th July–3rd August for the period 1979–1995; and the corresponding departures from those means for 15th July –3rd August, 2010 (d–f) and for 15th July–3rd August, 2011 (g–i). Analyses accessed from the web site of the Earth Systems Research Laboratory (http://www.esrl.noaa.gov/psd/data/histdata/).

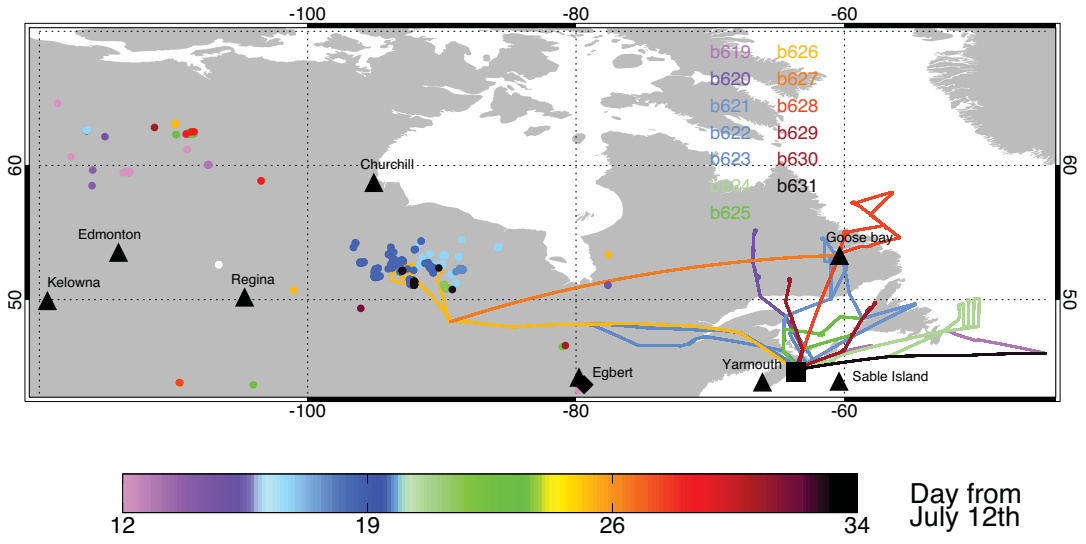

Fig. 4: Flight tracks for BORTAS, excluding inbound/outbound transit flights. Solid upward triangles denote ozonesonde launch sites, and the solid square denotes the Dalhousie ground station. The colour circles denote active burning throughout the BORTAS period. The flights and burning areas use a common colour scale that denote the day since 12th July 2011.

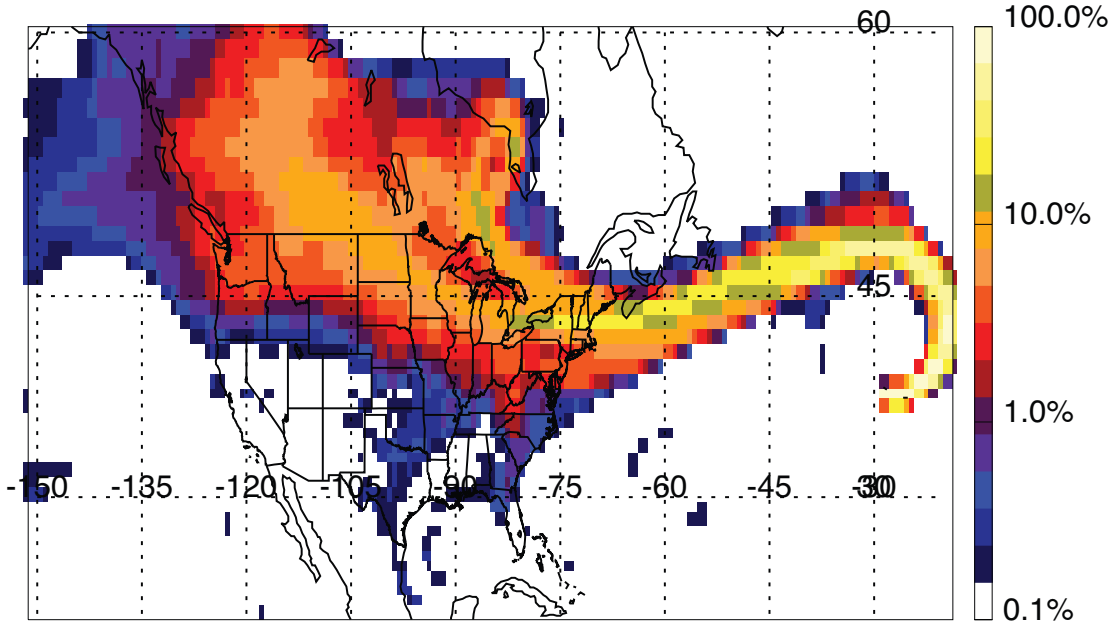

Fig. 5: Results for 13-day retroplumes with release times centered on 2100 UTC from the Pico Atmospheric Observatory between the altitudes of 2–2.5 km above mean sea level on the 24th July 2011. Percentage values reported represent the residence time, scaled by the maximum value in the meridional direction and vertically integrated. The mean altitude of this plume (not shown) was 4 km over the ocean and between 5–6 km over the contigious US and Canada.

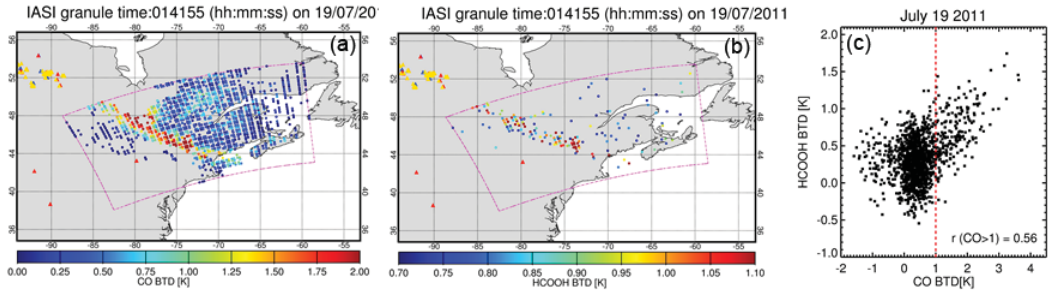

Fig. 6: Brightness temperature difference (BTD, K) detection of (a) CO and (b) formic acid (HCOOH) enhancements from a single IASI data granule for 19th July 2011. MODIS fire count data are shown as triangles according to detection certainty: high (red), nominal (yellow), and low (blue) confidence. (c) The corresponding scatterplot of CO and HCOOH with the Pearson correlation coefficient r shown inset.

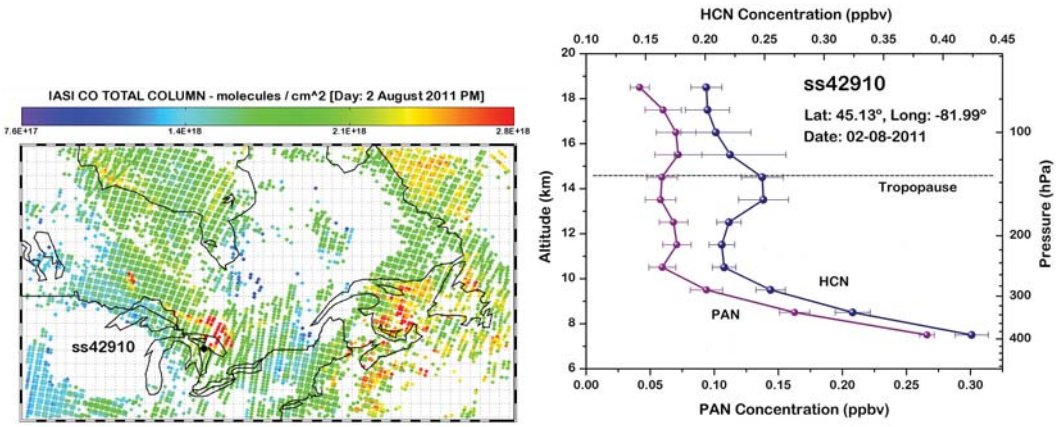

Fig. 7: Left: IASI total column CO (molec/cm^2) for 2nd August 2011. The black diamond superimposed denotes the position of occultation ss42910 from the ACE space-borne sensor. Right: vertical profiles of HCN (ppb) and PAN (ppb) from ACE during occultation ss42910 (45.13°N, -81.99°W).

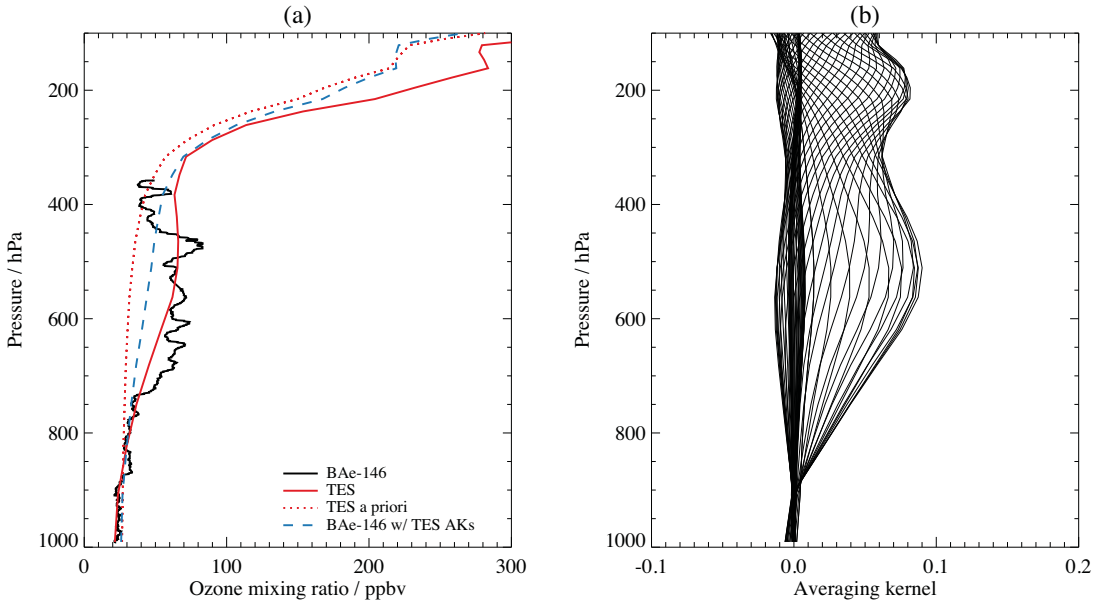

Fig. 8: Ozone profiles measured during a descent of the BAe-146 into Thunder Bay, ON on 26th July 2011. Plot (a) shows the O_3 profile measured from the BAe-146 (solid black line), retrieved from the collocated TES measurements and its prior (solid and dotted red lines, respectively), and the aircraft profile smoothed with the TES averaging kernels. Plot (b) shows the averaging kernels for the TES O_3 profile retrieval.

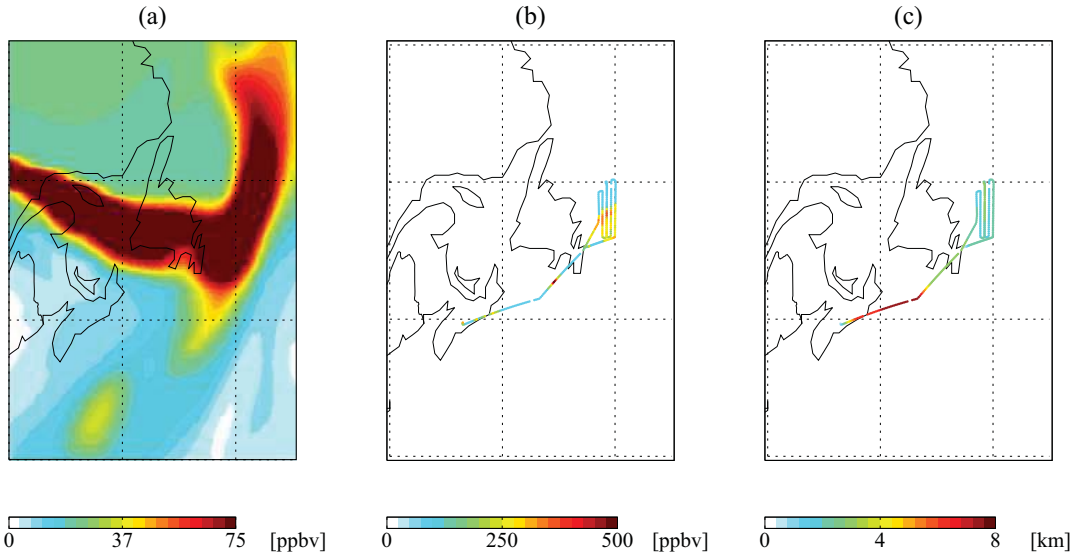

Fig. 9: (a) GEOS-5 model CO concentration (ppb) forecast for 1930Z at 750 hPa (initialized at 00Z on the same day), (b) BAe-146 aircraft CO measurements (ppb) and (c) altitude (km) for flight B624, 21st July 2011.

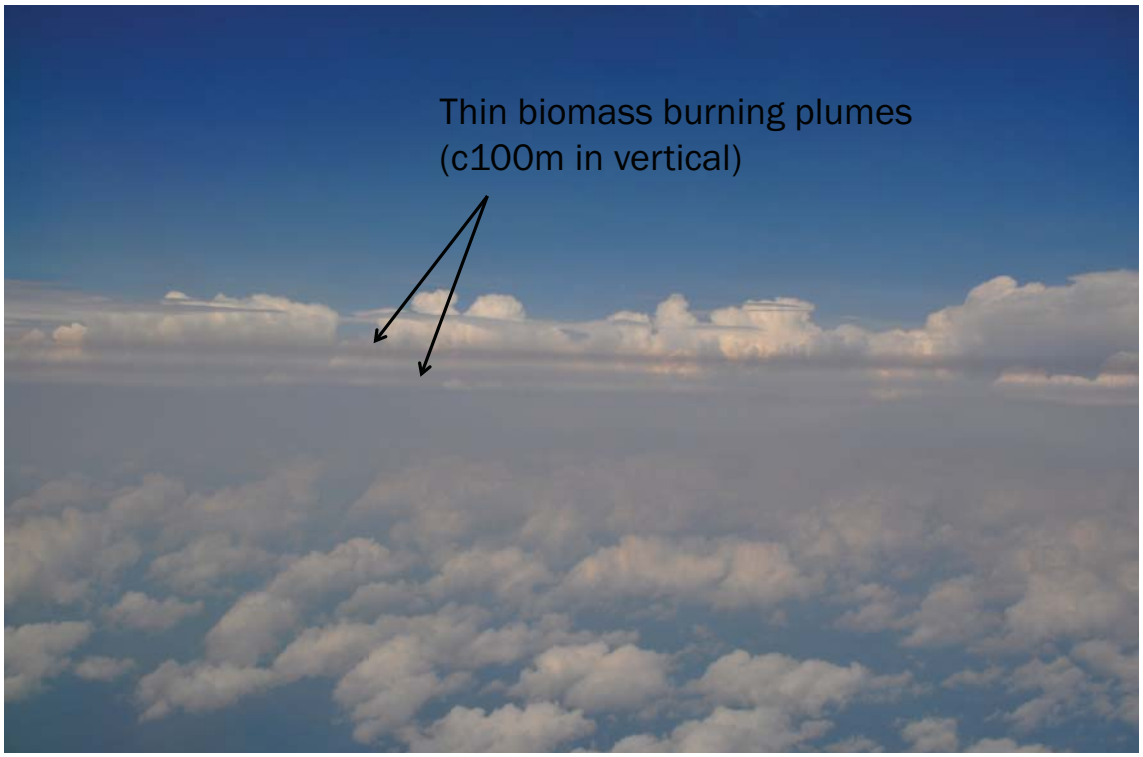

Fig. 10: A photograph (c/o Steve Andrews) from the BAe-146 at c7 km altitude during BORTAS-B (flight B624, 21st July 2011) illustrating the thin filaments of pyrogenic outflow.

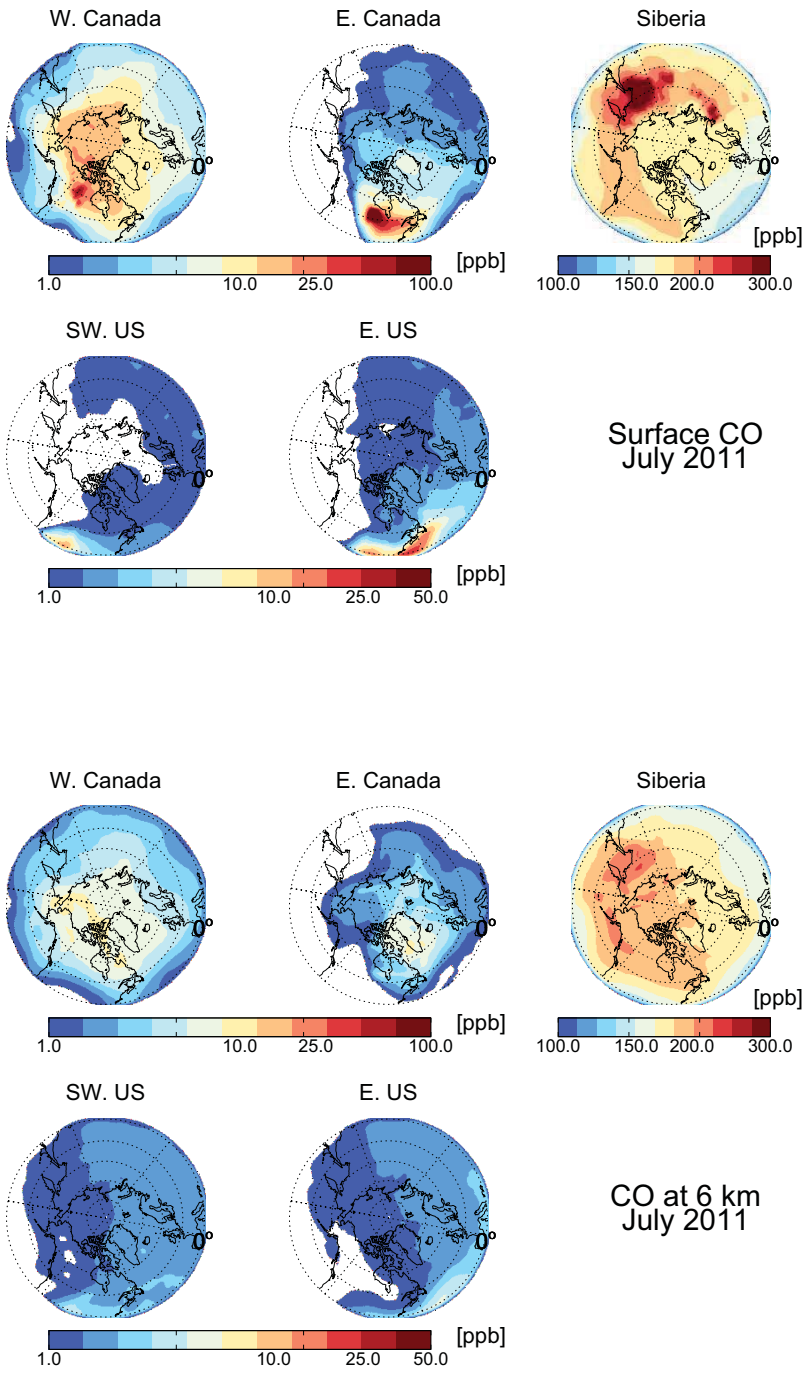

Fig. 11: Monthly mean GEOS-Chem global 3-D chemistry model output for July 2011 that describes pyrogenic contributions to total CO (ppb) from Western Canada, Eastern Canada, Siberia, Southwest contiguous US and Eastern contiguous US. The upper (lower) panel shows CO concentration at the surface (6 km).

Table 4: Ground-based measurements at the Dalhousie Ground Station during BORTAS.

Parameters	Instrument	Reference/Affiliation
Weather station	Temperature, dewpoint temperature, RH, wind direction and speed, rain amount, barometric pressure	Environment Canada,
Profiles of aerosol and cloud extinction	Raman LiDAR, Nd:YAG laser pulsing at 532 nm at 20 Hz	Dalhousie University, Bitar et al. (2010)
Partial columns of CO, CH_4, N_2O, C_2H_6, O_3	Dalhousie Atmospheric Observatory ABB Bomem DA8 FTIR Spectrometer measuring 750-4300 cm^{-1} with a resolution of 0.004 cm^{-1}.	Dalhousie University
Black carbon	Two-wavelength Magee AE22 aethalometer	Dalhousie University, Gibson et al. (2012)
$PM_{2.5}$, $PM_{2.5-10}$,	Teflon filter samples using Thermo Partisol 2025-dichotomour sampler. Filters analyzed for mass (gravimetric) and elements (energy dispersive x-ray fluorescence)	Dalhousie University, Gibson et al. (2009)
$PM_{2.5}$ anions and cations $PM_{2.5}$ organics, wood smoke marks, and OC/Elemental C	Nylon filter samples using Thermo ChemComb with integrated denuder to prevent positive sulphate artifacts. Nylon filters analyzed by ion chromotograph.	Dalhousie University, Gibson et al. (2012)
Total columns of CO, CH_4, O_3, N_2O	Portable Atmospheric Research Interferometric Spectrometer for the Infrared (PARIS-IR) measuring solar absorption spectra in the mid-IR (750–4400 cm^{-1}) at a resolution of 0.02 cm^{-1}	University of Toronto, Fu et al. (2007)
Aerosol number concentrations (20–500 nm, over 6 channels)	TSI 3031 Ultrafine Particle (UFP) Monitor (20–30 nm, 30–50 nm, 50–70 nm, 70–100 nm, 100–200 nm, 200–500 nm)	Environment Canada,
Aerosol number concentrations (500 nm–20μm, over 52 channels)	TSI 3321 Aerodynamic Particle Size (APS)	Environment Canada,
Aerosol ion characterization (10 nm–18 μm, over 12 size ranges)	MSP Micro-orifice Uniform Deposit Impactor (MOUDI) 100/110NR for sulphate, nitrate, sodium, chloride, ammonium, and pH	Environment Canada, Marple et al. (1991)
Aerosol speciation (40 nm–1 μm)	Aerodyne Aerosol Chemical Speciation Monitor (ACSM) Ammonium, organics, sulphate, nitrate, chloride	Environment Canada, Ng et al. (2011)
O_3	UV photometric analyzer Thermo Scientific 49i	Environment Canada,
Aerosol optical thickness	AERONET Sun Photometer 340, 380, 440, 500, 675, 870, 1020, 1640 nm	Dalhousie University Holben et al. (1998)
Aerosol optical thickness	Star photometer (418.3, 449.4, 469.2, 500.1, 532.4, 551.3, 607.6, 641.9, 679.0, 755.1, 783.3, 868.0, 939.9, 950.3, 959.9, 1033.8 and 1048.5 nm) Precision accuracy $0.003 < \Delta\tau < 0.011$	U. Sherbrooke Leiterer et al. (1995)

Table 5: Chemical and physical atmospheric observations at the Pico Mountain Observatory during BORTAS A and B.

Measurement	Method/Instrumentation
Meteorological variables	Commercial sensors for temperature, relative humidity, wind speed and direction
O_3	UV Absorption, Thermoenvironmental Corp. Model 49C
CO	NDIR, Thermo Environmental, Inc., Model 48C-TL
NO, NO_2, NO_y*	Custom-built Chemiluminescence Instrument
NMHCs	Custom-built Preconcentration System with GC-FID
Black carbon	Aethalometer, Magee Scientific Model AE31
Particle size	Intracavity Optical Particle Sizer/PMS LAS-X
CH_4, N_2O, SF_6, CO, CO_2, NMHC, CO_2 and CH_4 stable isotopes	Whole Air Sample Collection into Glass Flask Samples with susequent analysis at NOAA-GMD, USA

* Not available in 2011.

Table 6: Range of photochemical ages of airmasses, identified as of pyrogenic origin using CO, CH_3CN and HCN concentrations, intercepted during non-transit BORTAS-B flights, 15th July–31st July, 2011.

Flight #	Photochemical Age (days)
B620	-
B621	Typically 3–4, few older
B622	Typically 1–5, few younger and older
B623	Typically 2–4, few older
B624	Typically 2–4, few younger and older
B625	-
B626	$\geq$5 earlier in flight, 1–2 later in flight
B627	-
B628	Typically 8–11
B629	Typically 5–8
B630	Typically 5–9